Pacific Northwest
NATIONAL LABORATORY

PNNL-37567

Low Yield Nuclear Monitoring Physics Experiment 1 – Integrated Data Acquisition System Design and Initial Observations

October 2024

Christopher E. Strickland
Dorothy C. Linneman
James M. Knox
Dana Sirota
PE1 Experiment Team*

U.S. DEPARTMENT OF ENERGY

Prepared for the U.S. Department of Energy
under Contract DE-AC05-76RL01830

DISCLAIMER

PACIFIC NORTHWEST NATIONAL LABORATORY
operated by
BATTELLE
for the
UNITED STATES DEPARTMENT OF ENERGY
under Contract DE-AC05-76RL01830

Printed in the United States of America

Available to DOE and DOE contractors from
the Office of Scientific and Technical Information,
P.O. Box 62, Oak Ridge, TN 37831-0062
www.osti.gov
ph: (865) 576-8401
fox: (865) 576-5728
email: reports@osti.gov

Available to the public from the National Technical Information Service
5301 Shawnee Rd., Alexandria, VA 22312
ph: (800) 553-NTIS (6847)
or (703) 605-6000
email: info@ntis.gov
Online ordering: http://www.ntis.gov

PNNL-37567

Low Yield Nuclear Monitoring Physics Experiment One – Integrated Data Acquisition System Design and Initial Observations

October 2024

Christopher E. Strickland
Dorothy C. Linneman
James M. Knox
Dana Sirota
PE1 Experiment Team*

Prepared for
the U.S. Department of Energy
under Contract DE-AC05-76RL01830

Pacific Northwest National Laboratory
Richland, Washington 99354

*** PE1 Team**

Myers, S.C.[1], Abbott, G.[6], Alexander, T.[2], Alger, E.[1], Alvarez, A.[5], Antoun, T.[1], Graham, A.[6], Banuelos, H.[5], Barela, M.[3], Barnhart, T.[3], Barrow, P.[4], Bartlett, T.[5], Bockman, A.[1], Bodmer, M.[4], Bogolub, K.[7], Bonner, J.[11], Borden, R.[4], Boukhalfa, H.[3], Bowman, D.[4], Britt, C.[2], Broman, B.[9], Broome, S.[4], Brown, B.[5], Burghardt, J.[2], Chester, D.[6], Choens, C.[4], Chojnicki, K.[2], Churby, A.[1], Cole, J.[3], Coleman, T.[9], Collard, J.[6], Couture, A.[2], Crosby, G.[1], Cruz-Cabrera, A.[4], D'Saint Angelo, D.[5], Walter, D.[1], DeVisser, B.[5], Dietel, M.[5], Downs, C.[4], Downs, N.[5], Dzenitis, E.[1], Eckert, E.[5], Eras, S.[4], Euler, G.[3], Ezzedine, S.[1], Fast, J.[2], Feldman, J.[2], Featherston, K.[5], Foxe, M.[2], Freimuth, C.[5], Fritz, B.[2], Galvin, G.[6], Gamboa, S.[5], Garner, L.[5], Gascoigne, T.[5], Gastelum, J.[2], Gaylord, J.[1], Gessey, D.[5], Glasgow, B.[2], Glomski, A.[1], Goodwin, M.[6], Green, D.[6], Griego, J.[4], Grover, S.[5], Gutierrez, J.[3], Haas, D.[8], Hall, R.[3], Hall, A.[1], Hardy, D.[5], Hauk, D.[2], Heath, J.[4], Holdcroft, J.[6], Holland, A.[4], Honjas, W.[7], Howard, K.[3], Hudson, C.[8], Ingraham, M.[4], Jaramillo, J.[4], Jenkins, A.[6], Johnson, C.[2], Jones, K.[4], Falliner, J.[4], Junor, W.[3], Keillor, M.[2], Kent, G.[7], Keogh, M.[5], Kibikas, W.[4], Leadbeater, K.[6], Knox, H.[2], Knox, J.[2], Kuhlman, K.[4], Kwiatkowski, C.[3], Laintz, K.[3], Lapka, J.[8], Larotonda, J.[5], Layne, J.[3], Ledoux, N.[3], Li, S.[3], Linneman, D.[2], Lipkowitz, P.[5], Malach, A.[4], MacLeod, G.[3], McCann, E.[2], McCombe, R.[3], Meierbachtol, C.[3], Mellors, R.[1], Memmot, B.[5], Mendenhall, W.[9], Mendez, J.[2], Miller, X.[5], Miller, A.[5], Miranda, F.[5], Montano, M.[4], Moore, M.[2], Morris, J.[1], Munley, W.[2], Murillo, E.[5], Musa, D.[3], Myers, T.[4], Navarro, A.[2], Nippress, S.[6], Otto, S.[3], Peacock, S.[6], Pemberton, S.[3], Perea, R.[2], Peterson, J.[2], Le Bas, P.[3], Plank, G.[7], Podrasky, A.[9], Podrasky, D.[9], Pope, J.[4], Poskey, M.[5], Powell, M.[4], Price, A.[1], Puyleart, A.[2], Quintana, B.[3], Rahn, T.[3], Rendon, C.[5], Reppart, J.[5], Rico, H.[5], Roberts, B.[4], Robey, E.[4], Rodd, R.[1], Rodriguez, M.[4], Rogall, A.[3], Romanczuk, A.[1], Roth, M.[2], Salyer, G.[5], Savran, B.[7], Schalk, W.[10], Seifert, C.[2], Seitz, D.[3], Shao, X.[3], Sirota, D.[2], Slack, J.[2], Slater, D.[7], Smith, K.[7], Smith, D.[5], Spears, B.[3], Sprinkle, D.[2], Stead, R.[3], Stephens, M.[5], St Clair, J.[2], Strickland, C.[2], Tafoya, A.[3], Tafoya, J.[4], Tagoe, M.[5], Taguba, C.[2], Tarnecki, L.[3], Tatge, R.[5], Teich-McGoldrick, S.[4], Terry, B.[6], Thompson, R.[5], Townsend, M.[5], Tubbs, G.[3], Turley, R.[5], Valdez, N.[4], Van Morris, A.[2], Vergara, S.[5], Vigil, J.[3], Villanueva, J.[5], Vorobiev, O.[1], Wallace, D.[3], Walrath, T.[3], Wharton, S.[1], White, R.[5], White, H.[6], Whitehill, A.[2], Williams, M.[4], Wilson, J.[4], Wood, L.[2], Wright, C.[3], Wright, A.[4], Xu, G.[4], Yang, X.[1], Yost, R.[3], Zeiler, C.[5], Zionce, E.[2]

[1] Lawrence Livermore National Laboratory
[2] Pacific Northwest National Laboratory
[3] Los Alamos National Laboratory
[4] Sandia National Laboratories
[5] Nevada National Security Site
[6] Atomic Weapons Establishment
[7] University of Nevada Reno
[8] University of Texas at Austin
[9] Silixa
[10] National Oceanic and Atmospheric Administration
[11] Desert Research Institute

Abstract

The report documents the design of the Integrated Data AcQuisition (IDAQ) system and observations recorded during the first in a series of underground chemical explosions conducted on the Nevada National Security Site (NNSS) in southern Nevada. Experiments are funded as part of Low Yield Nuclear Monitoring (LYNM) research and development within the United States National Nuclear Security Administration NA-22 nuclear non-proliferation program. The series is part of the broader Physical Experiment 1 (PE1) being conducted in and around the P-tunnel facility on the NNSS. Each explosive experiment utilizes several tons of comp-B to generate signals recorded by a broad suite of instrumentation. The IDAQ serves as the backbone for all subsurface instrumentation providing precise time synchronization, remote control, data exfiltration and backup, along with recording several sensing modalities throughout the underground complex that includes ground motion, environmental conditions, and electromagnetic signals.

Summary

Multiple signals can be observed during and after the detonation of an underground explosion that include pressure, temperature, ground motion (i.e. elastic motion, permanent deformation/damage), electromagnetic, and material transport (e.g. gases, liquids, and solutes) through porous and/or fractured media [Myers et al. 2024]. Each of the observed signals can be used to help improve understanding of fundamental processes and validate or refine numerical models used to simulate and predict effects from underground explosions.

The Low Yield Nuclear Monitoring (LYNM) Physics Experiment 1 (PE1) seeks to design, build, and execute a series of experiments that will collect data from multiple sensing modalities with the goal of better understanding underground explosions. A description of the full set of LYNM PE1 experiments can be found in *Myers et al. 2024.* This report will focus on subsurface instrumentation and in particular the Integrated Data AcQuisition (IDAQ) system that was utilized for the first explosive experiment, also referred to as experiment A. Each explosive experiment utilizes a broad suite of instrumentation. The IDAQ serves as the backbone for all subsurface instrumentation (i.e. sensors located within the underground facility) providing precise time synchronization, remote control, data exfiltration and backup, along with recording several sensing modalities throughout the underground complex that includes ground motion, environmental conditions, and electromagnetic signals. The report documents the design of the IDAQ system along with observations recorded for the experiment A chemical explosion that was conducted in the fall of 2023.

Acknowledgments

This Low Yield Nuclear Monitoring (LYNM) research was funded by the National Nuclear Security Administration, Defense Nuclear Nonproliferation Research and Development (NNSA DNN R&D). The authors acknowledge important interdisciplinary collaboration with scientists and engineers from LANL, LLNL, NNSS, PNNL, and SNL.

PE1 Team in front of U12p-tunnel portal

Contents

Figures

Tables

1.0 Introduction

1.1 Setting

The location for the Low Yield Nuclear Monitoring (LYNM) Physics Experiment 1 (PE1) experiments is in Southern Nevada at the Nevada National Security Site (NNSS) managed by the United States National Nuclear Security Administration (NNSA), specifically within and surrounding the U12p-tunnel (P-tunnel) facility. The site is home to previous underground explosive experiments and provides a unique setting for PE1. The geology in the vicinity of the experiments consists of multiple tuff units (Figure 1**Error! Reference source not found.**).

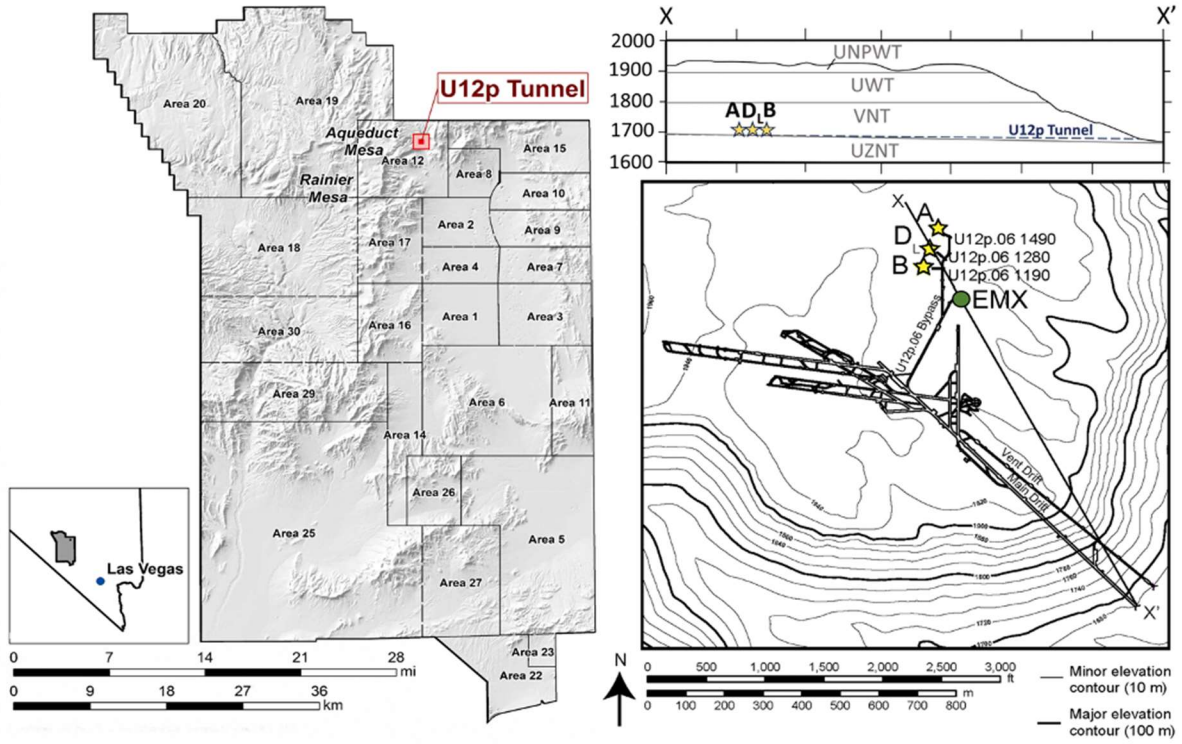

Figure 1 Map showing the NNSS, P-tunnel facility, primary geologic units, and locations of the three explosive experiments (A, B, and DL). Reproduced from Myers et al. 2024

The Integrated Data AcQuisition (IDAQ) system serves as the backbone for all subsurface instrumentation and consists of several nodes and remote workstations interconnected using a fiber-optic network located within both the underground and on the apron of the P-tunnel facility (Figure 2).

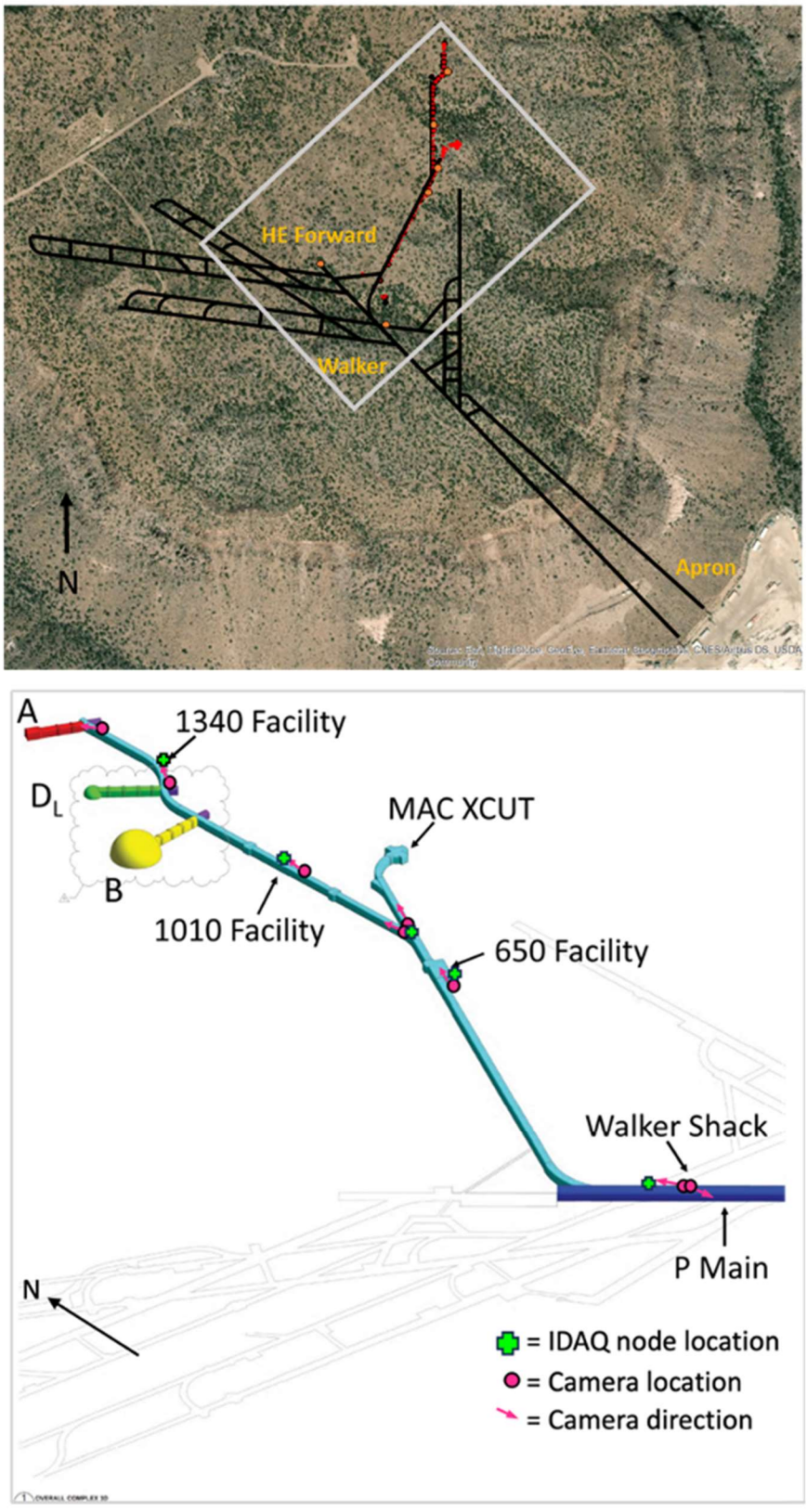

Figure 2 Map of IDAQ locations in the P-tunnel facility

2.0 IDAQ Design

2.1 Motivation

Underground settings present unique challenges for complex multidisciplinary experiments. Lessons learned from previous underground experimental efforts, most recently the EGS Collab project conducted at the Sanford Underground Research Facility (SURF) (Figure 3), have been leveraged to help guide the instrument design for LYNM PE1. Primary factors that impact experiments are 1) satellite and cellular signals cannot penetrate the overlying rock to provide for time synchronization or data exfiltration, 2) underground environments exhibit high humidity and dust that enhances damage to sensitive electronics, and 3) access is often much more difficult relative to surface sites limiting the ability for research and support staff to install, test, maintain, and operate experimental equipment.

The IDAQ was designed to overcome previously identified difficulties and provide a robust backbone supporting precise time synchronization, remote instrument control, data exfiltration, and data backup, enabling the effective integration of multiple instrumentation teams conducting underground experiments.

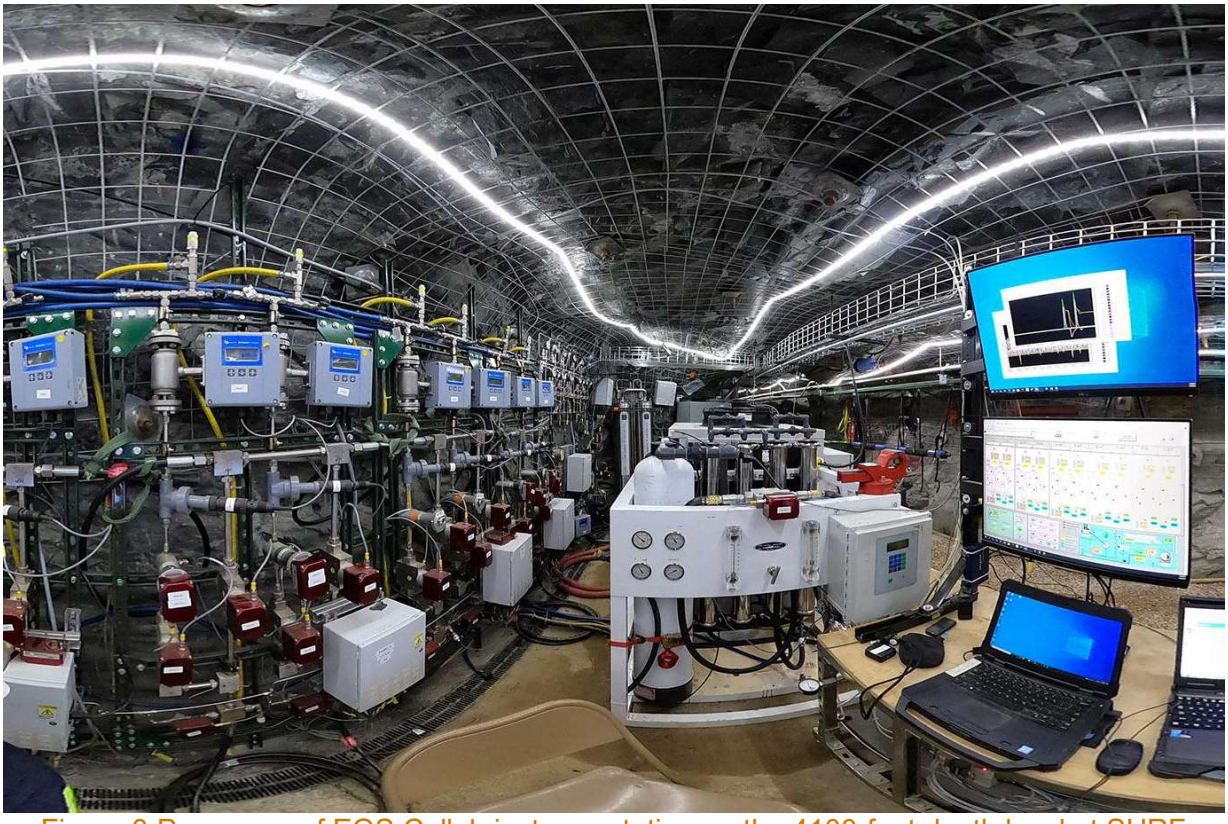

Figure 3 Panorama of EGS Collab instrumentation on the 4100-foot depth level at SURF

2.2 Design Elements

The IDAQ acts as the integration point for various project elements (Figure 4). Time synchronization is provided through two redundant subsystems: 1) network time, and 2) a timing fiducial provided by the high explosives team coincident with the signal sent to fire the explosive

stack (i.e. HE-trigger signal). Each of the subsurface instrumentation teams installed equipment that recorded data for their specific modality. The IDAQ connects those underground systems to locations on the apron (just outside the portals to the underground P-tunnel facility) where staff can access underground equipment for control, data exfiltration, and data visualization.

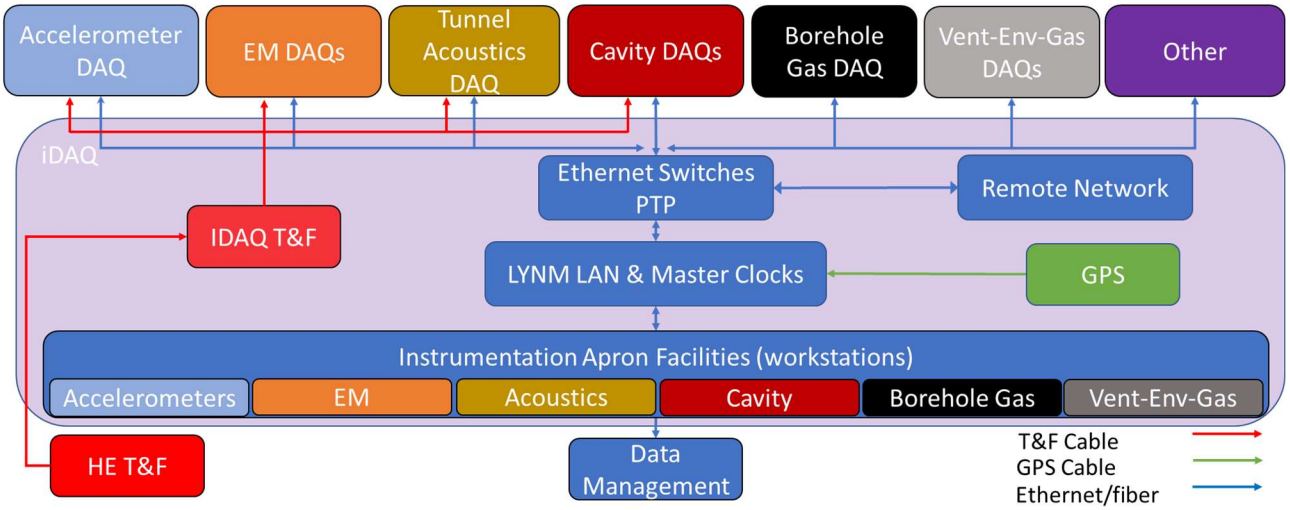

Figure 4 Functional block diagram illustrating the relationship between IDAQ and other project teams: Drift & borehole accelerometers, electromagnetics (EM), tunnel acoustics, cavity, borehole gas circulation, ventilation (vent) & drift environmental (env) gas, and high explosives (HE). T&F denotes timing and firing systems, PTP precision time protocol, GPS global positioning system, and LAN local area network

2.2.1 Harsh Environment Protection

Underground environments often present harsh conditions that can accelerate damage to sensitive experimental instruments. Dust, high moisture, and facility operations (e.g. mining, digging, rock bolting) at P-tunnel all result in challenging environment conditions. To minimize the damage, the IDAQ node enclosures were designed to be dust and moisture resistant (Figure 5). Thermal control relies on thermoelectric heater/chiller units (Rittal model 3201200). Each heater/chiller is equipped with two isolated fan units, one on either side of the thermoelectric heat exchanger. In this way outside air is not brought into the enclosure but provides for clean, temperature-controlled air circulation. All cable feedthroughs (fiber-optic, Ethernet, AC power, sensor signals) are designed to provide a liquid and gas tight seal. Cable connections exterior to the enclosure also have integral strain relief and armoring. At locations in the P.06 Bypass, accelerations due to the explosion shock wave were expected to exceed deign tolerances for some equipment. To reduce shock impacts on equipment, isolation systems were designed to limit accelerations to no more than 2g. For each IDAQ enclosure (SKB model 3SKB-R06U20W), elastomer shock damping was internally incorporated and wire-rope isolators (Vibrodynamics model HH series) were also installed between the ground and the base of each underground IDAQ node to limit shock impacts to internal components.

Figure 5 IDAQ node at MAC-Y location illustrating features used to protect from harsh underground environments

2.2.2 Data Exfiltration and Remote Control

A fundamental requirement for the PE1 experiments is to not only record each of the desired instrumentation datasets but ensure that none of the data are lost. A network that connects underground recording locations to workstations for instrument control, data visualization and backup must be properly designed and operated. The IDAQ local area network (LAN) backbone for PE1 consists of access points that use industrial grade managed switches (Cisco IE4000,Figure 6) interconnected using fiber optics in a redundant loop (Figure 7). Redundancy ensures that in the event a single interconnection, power supply, or switch is lost, the entire network will continue to seamlessly function.

Workstations for each instrumentation modality are staged in buildings on the P-tunnel facility apron and provide for remote control of all systems.

Figure 6 IDAQ LAN switch, redundant power supplies, and UPS

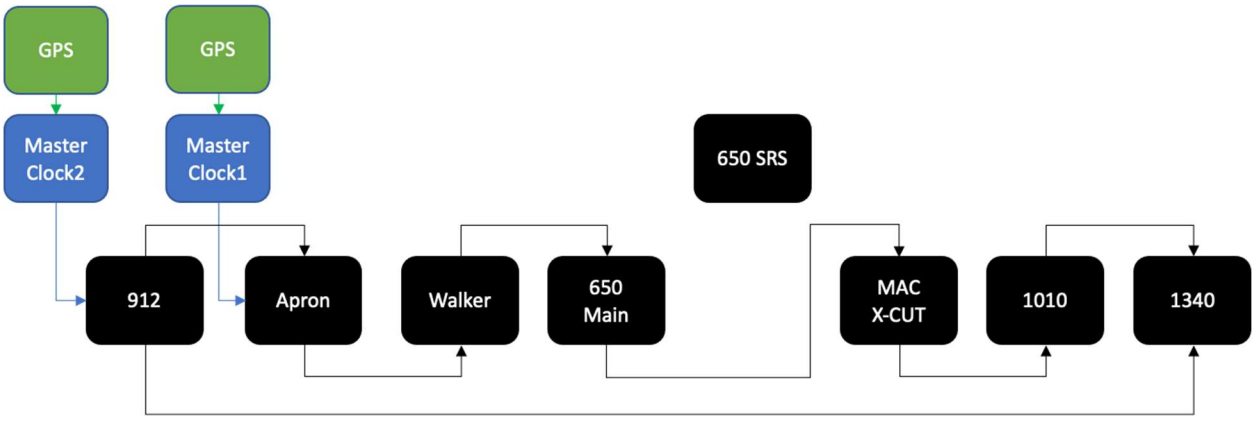

Figure 7 PE1 IDAQ LAN configuration

2.2.3 Time Synchronization

Time synchronization is accomplished through two independent systems. The primary method implements Precision Time Protocol (PTP) across the IDAQ (LAN) that can be used as a time reference by all instrumentation teams to achieve time synchronization to UTC with an accuracy of better than a microsecond. For instrumentation that do not require microsecond time synchronization, Network Time Protocol (NTP) is also implemented on the IDAQ LAN. A set of master clocks (Masterclock model GMR5000) are each synchronized to a constellation of GPS/GNSS satellites and configured to provide for redundancy if two out of three are lost. Low

drift Rubidium oscillators were chosen to ensure microsecond time synchronization even after several hours following loss of GPS lock.

In addition to PTP, an electronic pulse signal (i.e. trigger) is provided by the high explosive timing and firing (HE T&F) coincident with the firing signal sent to the explosive stack and can be used as a secondary timing fiducial. The IDAQ receives this trigger signal and distributes to all instrumentation located in the subsurface (Figure 8). In conjunction with the fiber optic backbone, trigger pulse signals are relayed using electrical-optical and optical-electrical converters (Highland Technologies models J720 and J730, Figure 9). For most underground locations only one or two trigger signals are required by instrumentation. However, a large portion of the underground instrumentation is located at the P.06 bypass 650 facility and requires the use of additional equipment. The 650 IDAQ node is paired with a second system (Stanford Research Systems model FS735, Figure 10) that receives the trigger signal and distributes to as many as 16 instrumentation devices at that location.

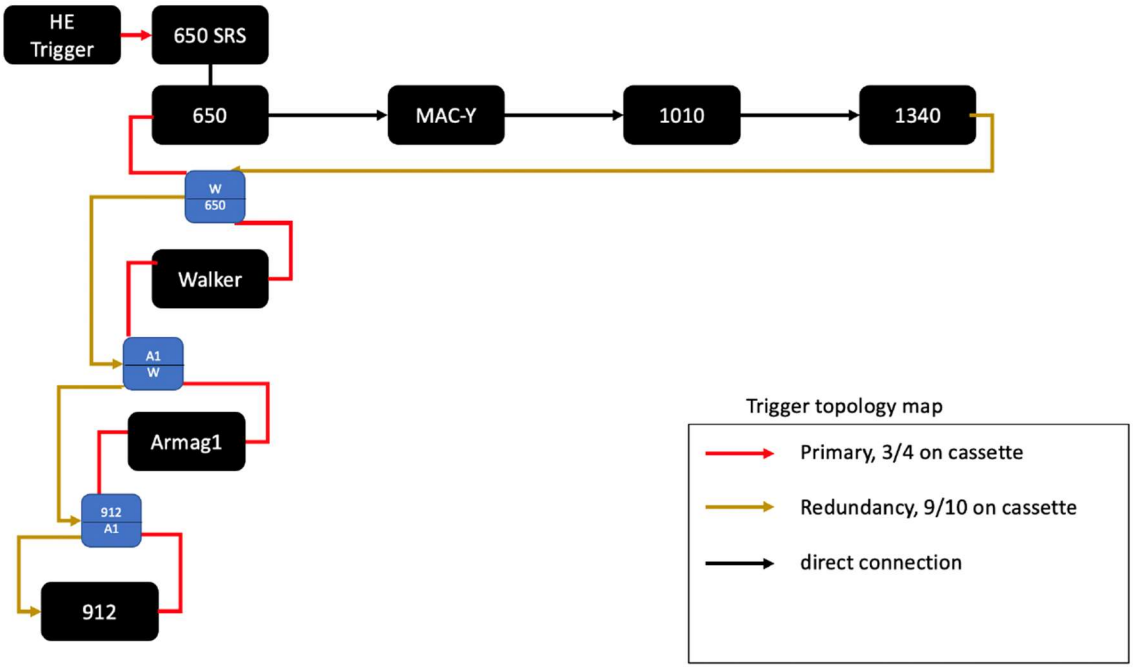

Figure 8 IDAQ trigger signal configuration

Figure 9 Electrical to optical and optical to electrical converters used for the PE1 IDAQ trigger distribution network

Figure 10 SRS distribution amplifier used for trigger relay at the P.06 bypass drift 650 facility

2.2.4 Power and Data Backup

Along with the use of redundant power supplies for LAN switches and sensor data acquisition systems, each IDAQ node is equipped with an uninterruptible power supply (UPS Tripp-lite model SU2200RTXL2U). Data from all instrumentation modalities, including IDAQ, is not only stored locally on each system but automatically backed up to a redundant array of independent disks (RAID) drive (Synology model SAMZ76P4T0BW) located on the apron using the IDAQ LAN (Figure 11). RAID backup frequency was different for each instrumentation modality and based on individual needs.

Figure 11 IDAQ ARMAG1 node containing master clock, RAID drive, and UPS

Power state is continuously monitored and recorded on each IDAQ node. Two conditions are monitored: power status (i.e. power on/off) and battery health (i.e. low battery). The UPS system is equipped with two relays that close if the respective power condition is met (Figure 12). The IDAQ monitors for the relay closures using an onboard data acquisition system (Campbell Scientific model CR310, Figure 13). If either the power is lost or the battery voltage falls below a set threshold, the system will automatically send an alarm to IDAQ personnel over both email and text message.

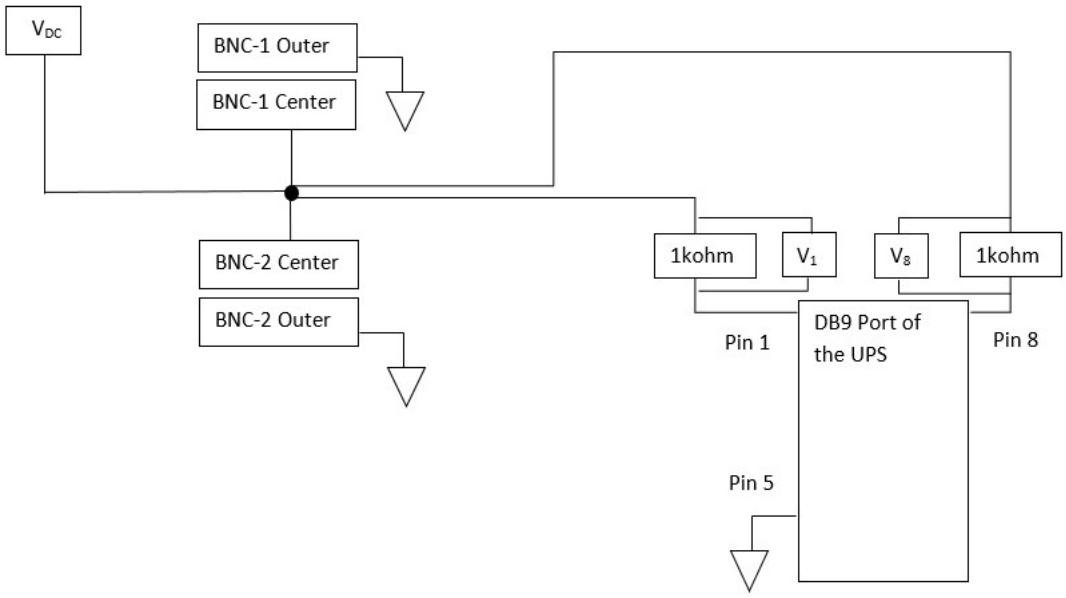

Figure 12 IDAQ UPS power state monitoring circuit and cable. BNC signal outer conductors are connected to instrumentation ground

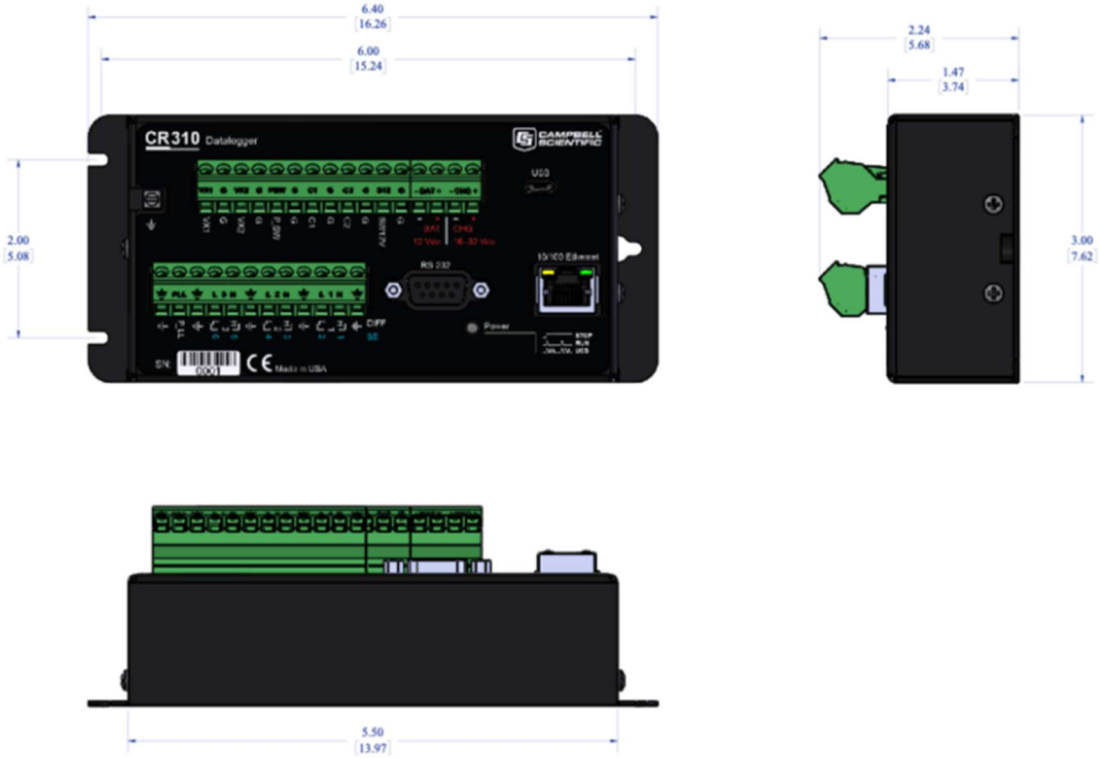

Figure 13 IDAQ data acquisition system for monitoring power and environmental conditions

2.2.5 Sensing

IDAQ nodes were designed with two data acquisition systems: low sample rate, <1 Sample/s; and high sample rates up to 20 MSamples/s. Low frequency DAQs record sensors that include UPS power and environmental conditions. High frequency DAQs recorded data from geophones, accelerometers, trigger signals, and electromagnetic sensors (Figure 14). The IDAQ was designed to be flexible so that additional sensor recording could be brought in and other DAQ modifications rapidly implemented if required by the project.

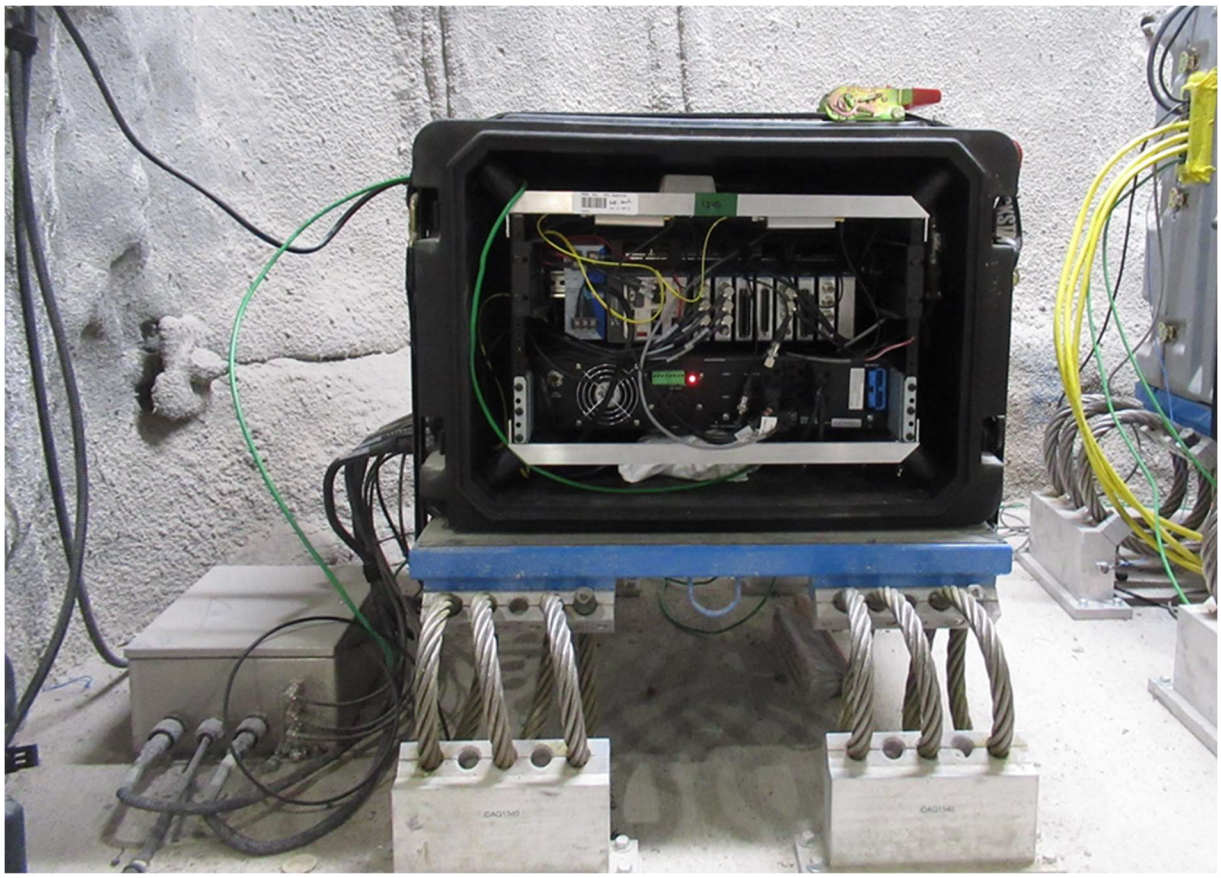

Figure 14 IDAQ node at P.06 bypass drift 1340 location showing the NI-cRIO DAQ and UPS within the enclosure and the interface box attached to the concrete pad on the left of the enclosure that contains fiber optic connections and ground motion sensors

2.2.5.1 Ground Motion

IDAQ ground motion sensors were designed to augment data acquired by other instrumentation teams. At each location, an accelerometer and geophone were installed onto an aluminum disk (1/2 inch thick, 4-inch diameter). The disk was machined with three outer holes used to level the assembly with set screws and a single hole in the center for rigid attachment to a concrete anchor set into the concrete pad (Figure 15) at each IDAQ location. The assembly was set into each interface box (Figure 16) prior to orienting to north, levelling, and anchoring which provided protection from the drift environment.

Figure 15 IDAQ ground motion sensors and mounting disk

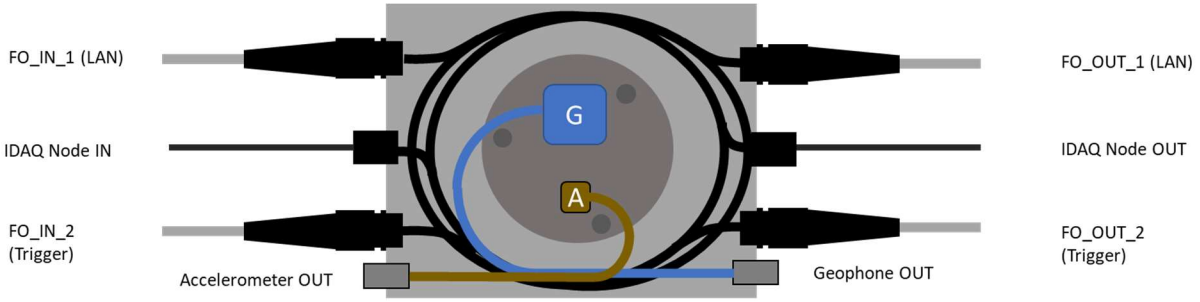

Figure 16 Schematic of the IDAQ interface box that contains ground motion sensors and fiber-optic interconnections

2.2.5.2 Drift Environmental Conditions

Drift conditions were monitored by the IDAQ low sample rate DAQ. Humidity and temperature were recorded both inside and outside of each IDAQ enclosure (Figure 17). Cameras were attached to each of the underground IDAQ nodes, shock mounted to the drift ribs and used to assess potential damage to instrumentation and the facility following the explosive experiment. At select locations, select gas concentration (i.e. ammonia), and drift air velocities were also recorded.

Figure 17 Humidity and temperature sensor used in each IDAQ node

2.2.5.3 Electromagnetics

The PE1 electromagnetics team installed a suite of sensors for recording both E-field and B-fields at two locations in the P.06 bypass drift. Triplets of stainless-steel electrodes coupled to the ground were installed to measure all three E-field components, both at high frequencies (>MHz) and low frequencies (< 50kHz). Three component B-field data were recorded using two different sensors, one for high frequencies and another for low frequency (Figure 18). In the week prior to the first explosive experiment the EM DAQ at the 1010 location failed. As mentioned earlier, the IDAQ has been designed to quickly adapt to such situations and was modified to acquire the low frequency E-field and B-field sensors.

Figure 18 Low frequency electromagnetic B-field, Phoenix Geophysics model MTC-150, sensor recorded by the 1010 IDAQ node

3.0 IDAQ Installation and Performance Testing

Installation of the IDAQ system at the P-tunnel facility began in the fall of 2021. Extensive testing in the laboratory occurred prior to field installation. Field testing was performed at several stages during and after installation and included interface testing with the high explosives and instrumentation teams followed by multiple dry runs.

3.1 Initial Laboratory Evaluations

3.1.1 IDAQ - High Explosives Systems Laboratory Integration Tests

One of the initial interface tests conducted was to evaluate time synchronization between the IDAQ and HE T&F systems in a laboratory setting. Timing systems from both teams were assembled at PNNL and run through a series of tests to quantify the quality of the synchronization. A schematic of the test configuration (Figure 19) and results (Figure 20) are provided below. The results suggest that the two systems should be able to achieve the required level of synchronization (better than one microsecond).

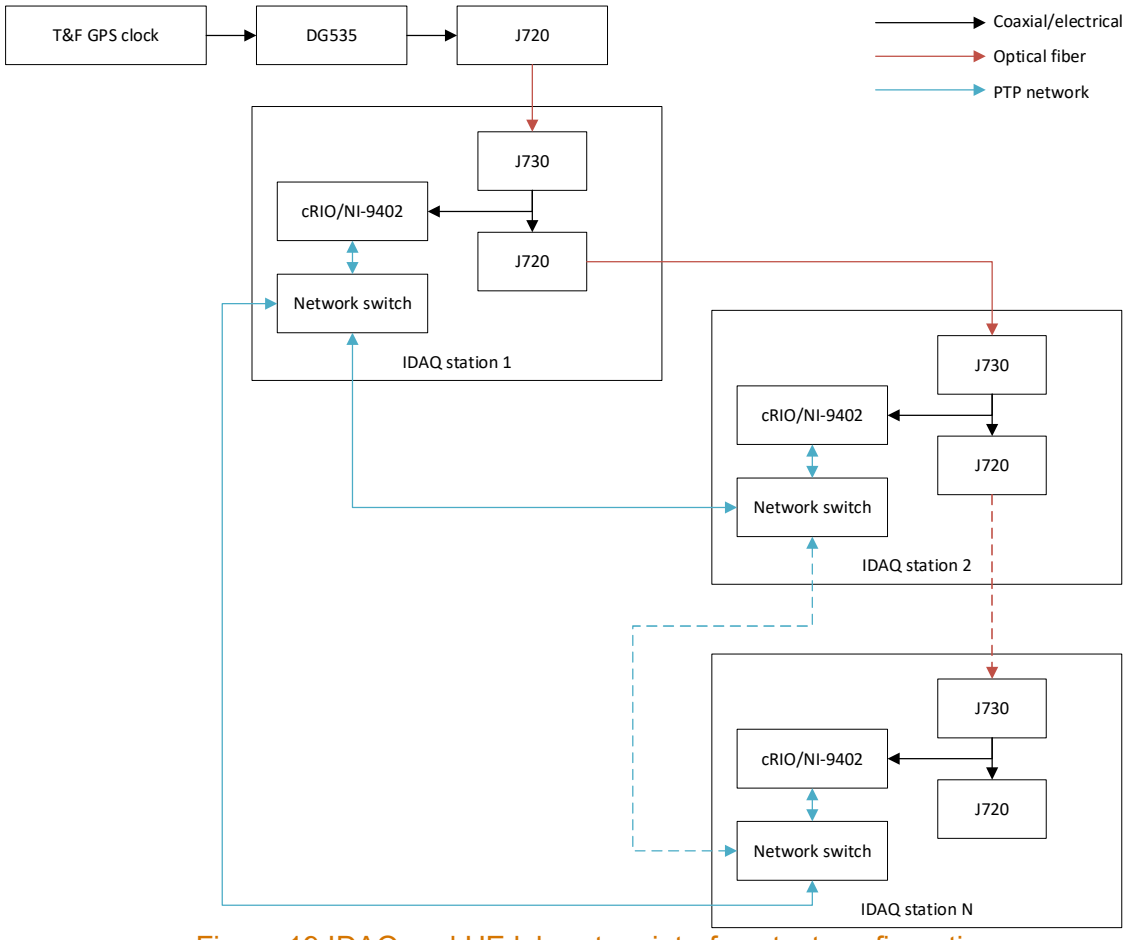

Figure 19 IDAQ and HE laboratory interface test configuration

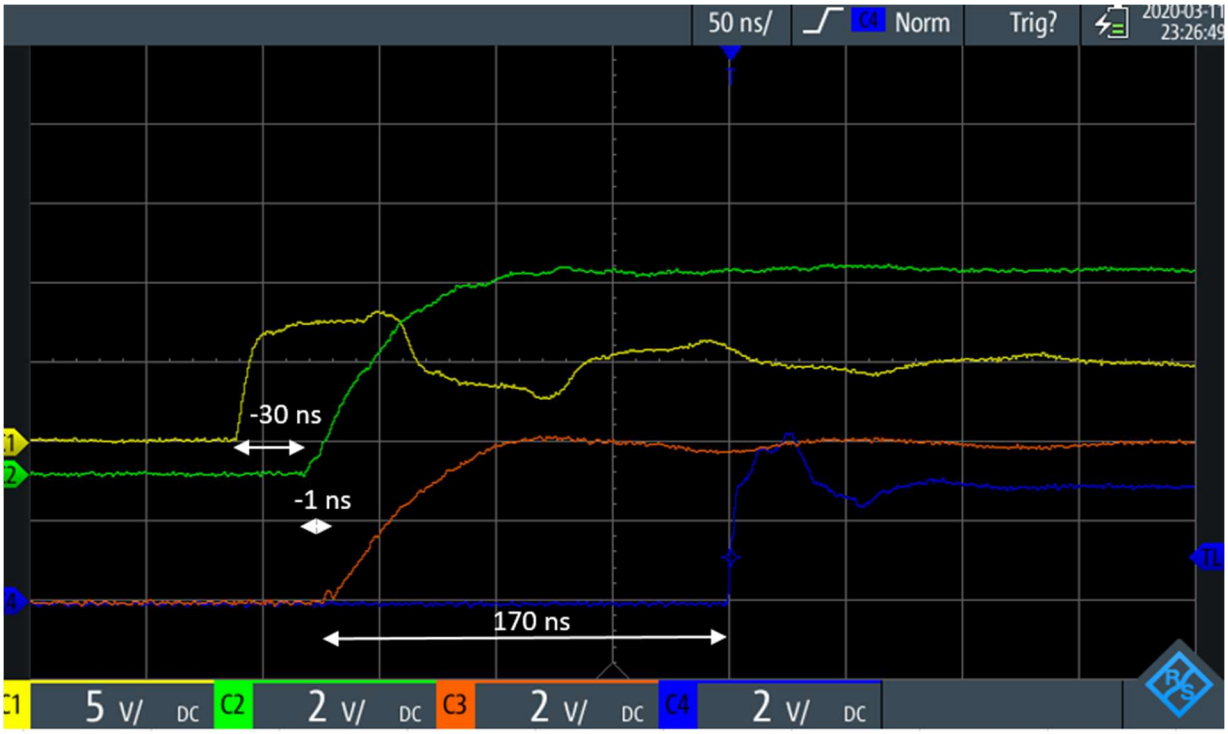

Figure 20 Test signals: Yellow is PPS signal from IDAQ clock; green is PPS signal from HE T&F clock; red is pulse out of the HE T&F clock-trigger; blue is the trigger received at the IDAQ NI-9402

3.2 Installation and Field Testing

Field installation began with the build out of the fiber-optic backbone required for both the IDAQ LAN and trigger systems. After the completion of the fiber-optic network, the IDAQ nodes were delivered to the site and installed. During installation both the LAN and trigger systems operations were thoroughly tested following similar procedures as laboratory testing. Troubleshooting of any observed initial issues and resolution occurred in parallel, and interface testing in the final field configuration was then performed.

3.2.1 Harsh Environment Protection

The IDAQ system was operated continuously for over two years prior to the first explosive experiment in October of 2023. Observations during that time showed the environmental control systems performed well. Little to no dust entered the enclosures (Figure 21) even though dust in the underground environment was quite high (Figure 22) and humidity never came close to exceeding design thresholds. Cabling interconnection also performed as designed and no breakage or degradation was observed.

Figure 21 Photos illustrating the level of dust reduction for the interior of IDAQ nodes relative to the environmental conditions outside

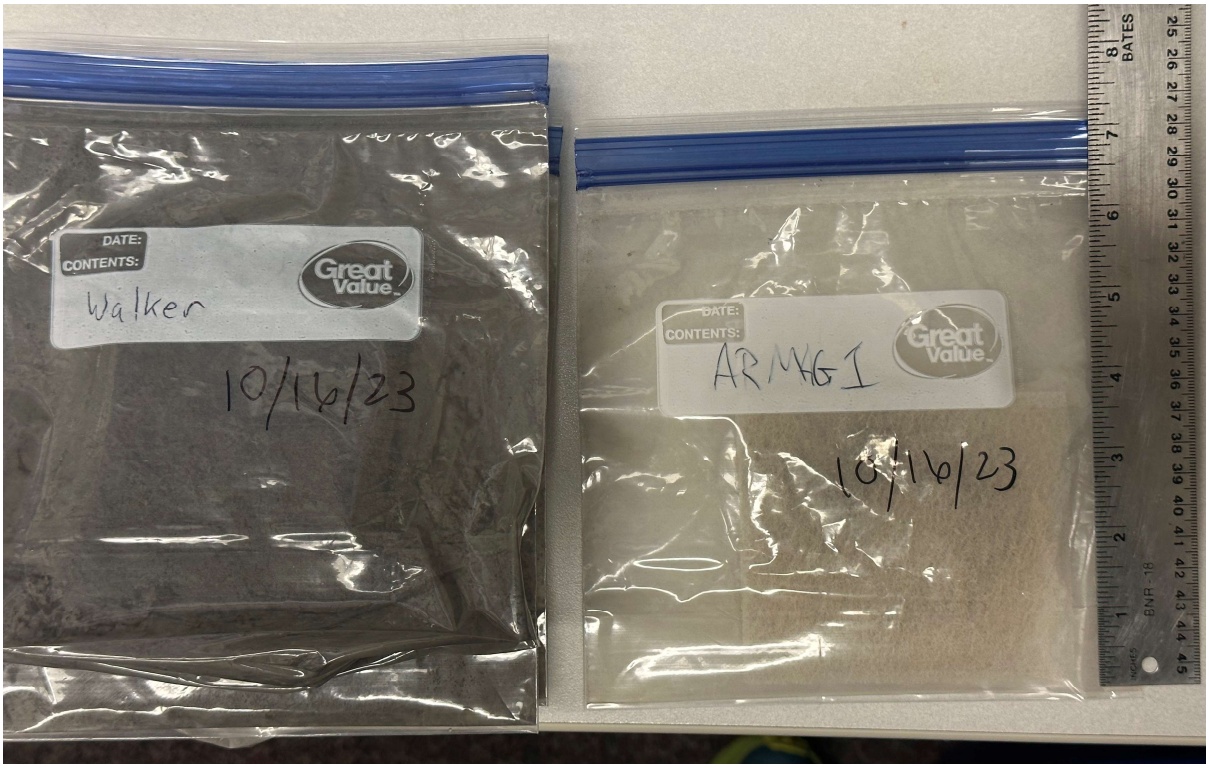

Figure 22 IDAQ thermal management system filter. Note the difference in dust/particulates collected for an underground (Walker) location relative to that of a node located outside on the apron (ARMAG1)

3.2.2 Data Exfiltration and Remote Control

Dry run testing provided opportunities to evaluate any limitations to data bandwidth during high exfiltration periods and potential effects on remote control from workstations on the apron. Many of the high-speed sensors that acquire data promptly after receiving the HE T&F trigger signal are configured to immediately begin sending that data across the IDAQ LAN. Results from the dry runs showed that the IDAQ LAN can exfiltrate all instrumentation data in just a few minutes after the trigger is received (Figure 23).

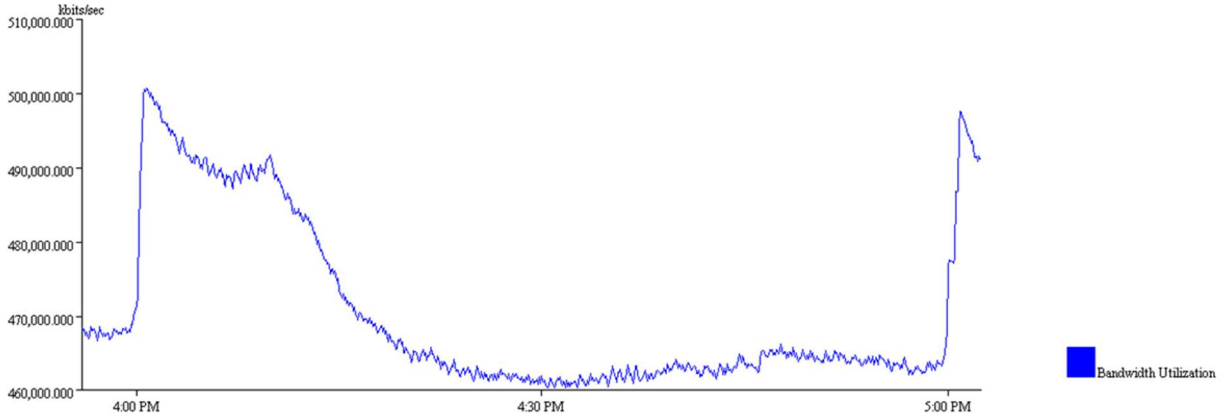

Figure 23 Increase in data utilization during dry runs. Maximum system bandwidth is 1Gbit/s

3.2.3 Time Synchronization

Time delays between all IDAQ nodes were determined using multiple methods. First, optical time domain reflectometer (OTDR) measurements were performed on each interconnection between adjacent IDAQ nodes and between the GPS antennas and master clocks. Each high speed IDAQ (National Instruments compact RIO model cRIO-9047) is synchronized to UTC using PTP and the relative time delay of the received trigger signal was recorded (National Instruments model NI-9402). Uncertainty in the time delays were determined by repeatedly sending trigger signals and calculating variations that were observed over time. Results show that the time synchronization uncertainty at all IDAQ nodes is much less than the one microsecond requirement (Table 1). Of note is that the time synchronization observed at Walker is much higher (~5x) than all other locations. The fiber-optic interconnection is much longer between that location and the apron and likely explains the larger uncertainty.

Both the IDAQ LAN and each of the master clocks were monitored using software provided by the respective vendors. LAN configuration, time synchronization to the master clock, and data bandwidth utilization were all continuously monitored during each of the dry runs (Figure 24). GPS lock, synchronization quality, number and identity of satellites, and detection of GPS jamming or spoofing was also monitored (Figure 25).

Table 1 Time delay measurements between IDAQ locations

Notes: Trigger signal begins at 650 -> MACX ->1010 -> 1340 -> B912 & apron infrastructure -> ARMAG1 -> Walker							
Time differences (ns)		**650**	**MACX**	**1010**	**1340**	**ARMAG1**	**Walker**
HE-Dry Run Mean travel time (ns)		0	375	1100	1700	12375	17820
Dry Run Mean travel time (ns)		0	415	1060	1685	12420	17630
Average travel time (ns)		0	395	1080	1693	12398	17725
Absolute Time Uncertainty (ns)		**0**	**28**	**28**	**11**	**32**	**134**

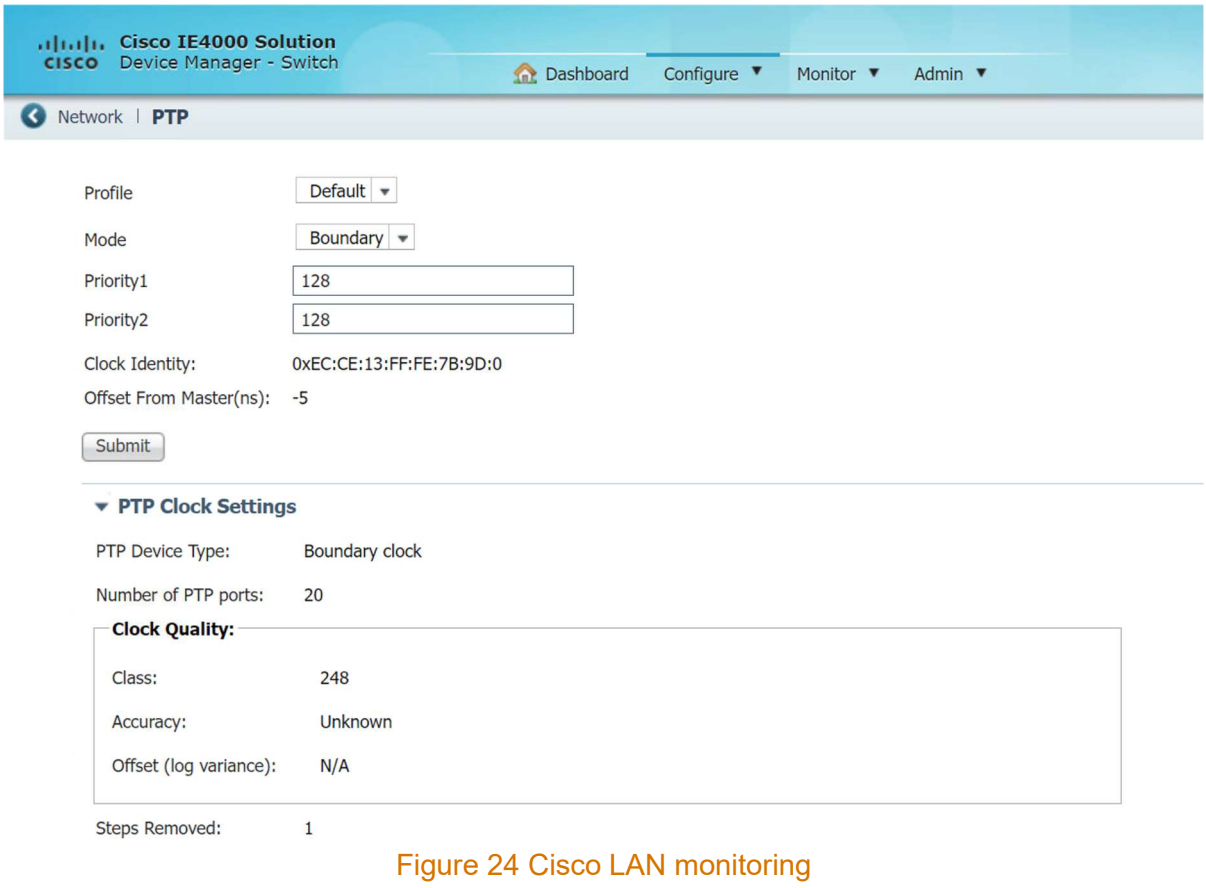

Figure 24 Cisco LAN monitoring

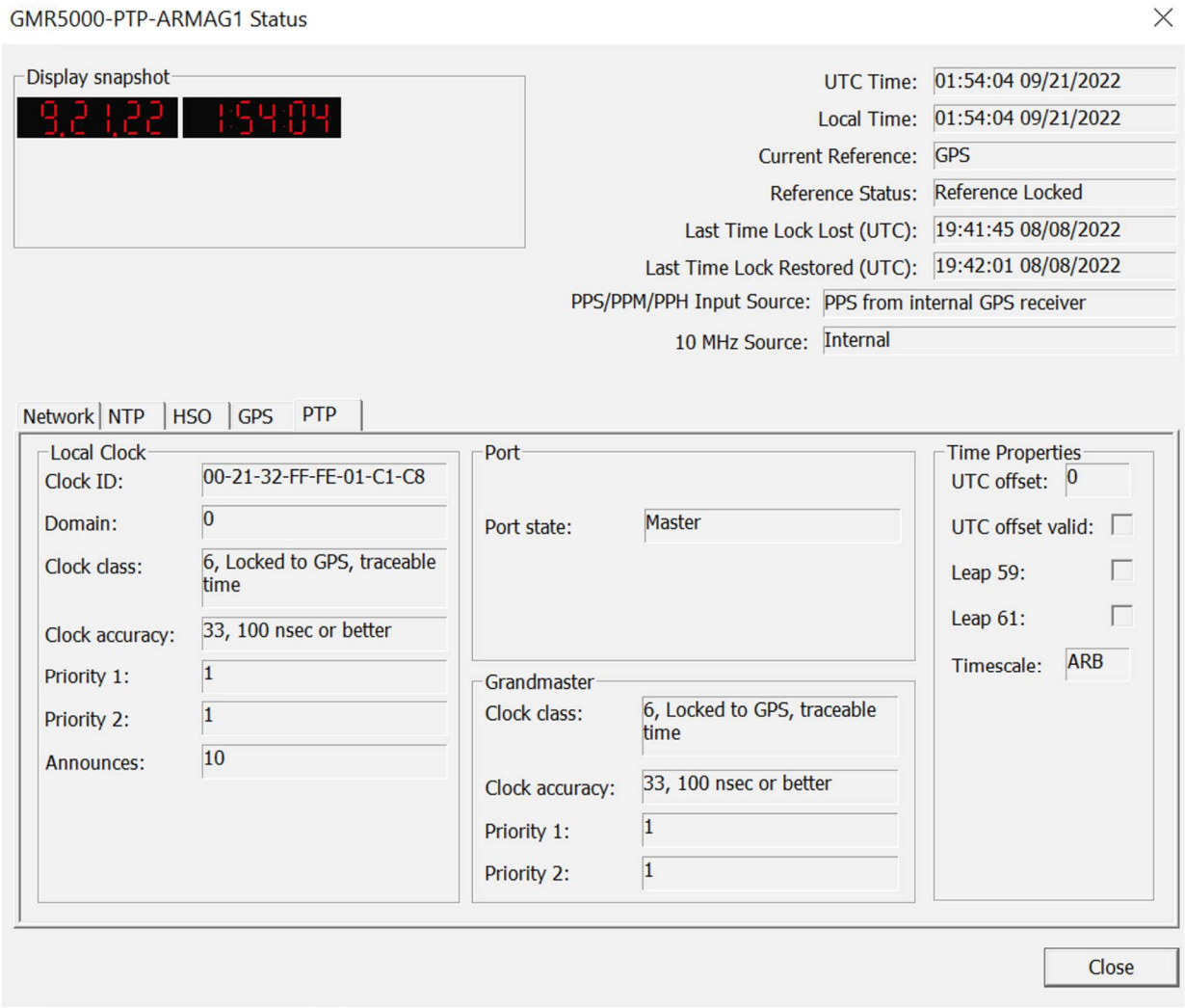

Figure 25 Master clock monitoring software

3.2.4 Power and Data Backup

IDAQ power state of health is continuously monitored and recorded. The number of seconds per minute an IDAQ node has lost power or exhibits a low battery condition is recorded to file and if an upset condition occurs, an email and text message alarm is sent to the IDAQ management team (Figure 26). Several power outages occurred, both planned and unplanned. The IDAQ UPS was shown to maintain operation for approximately 5 hours after loss of power and recover automatically after power is restored.

Data produced by each of the instrumentation and IDAQ teams is both recorded and saved locally to the respective DAQs and automatically copied to the network attached storage (NAS) RAID drive that is part of the IDAQ system (Figure 27). All data backup and automation routines are managed by the IDAQ team.

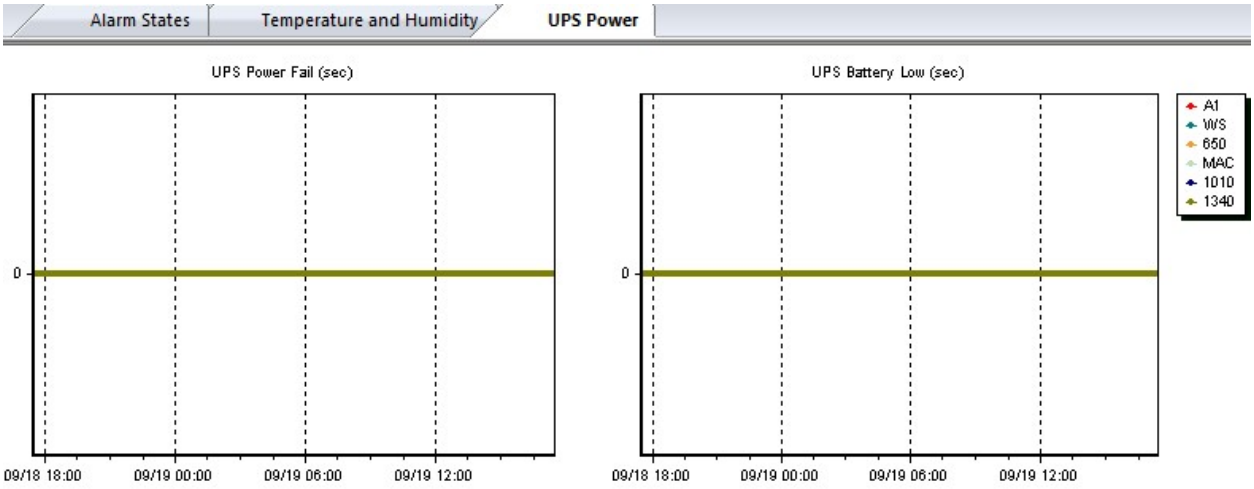

Figure 26 GUI for monitoring IDAQ power state of health

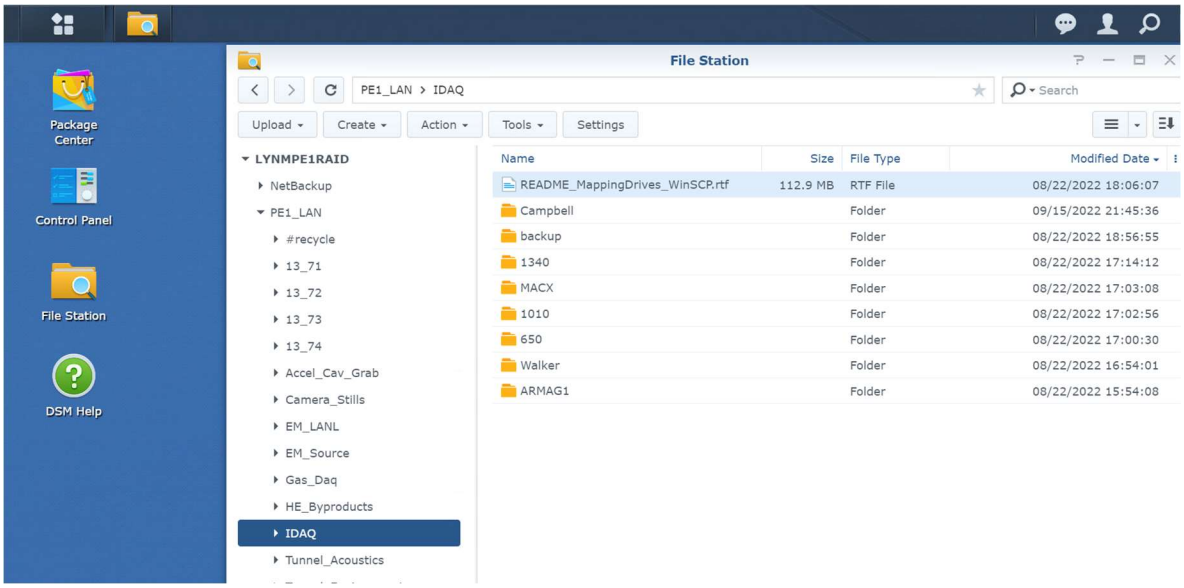

Figure 27 IDAQ RAID NAS software used for automated data backup

3.2.5 Ground Motion

The IDAQ was designed to record ground motion that results both directly from the explosive shock and subsequent aftershocks as the surrounding geologic media shifts or relaxes. Testing of the ground motion sensing was performed multiple times and included the use of explosive detonator tests (Figure 28), HE T&F ringdown tests using simple resistive loads, ground hammer strikes, as well as ambient noise assessments (Figure 29 - Figure 32).

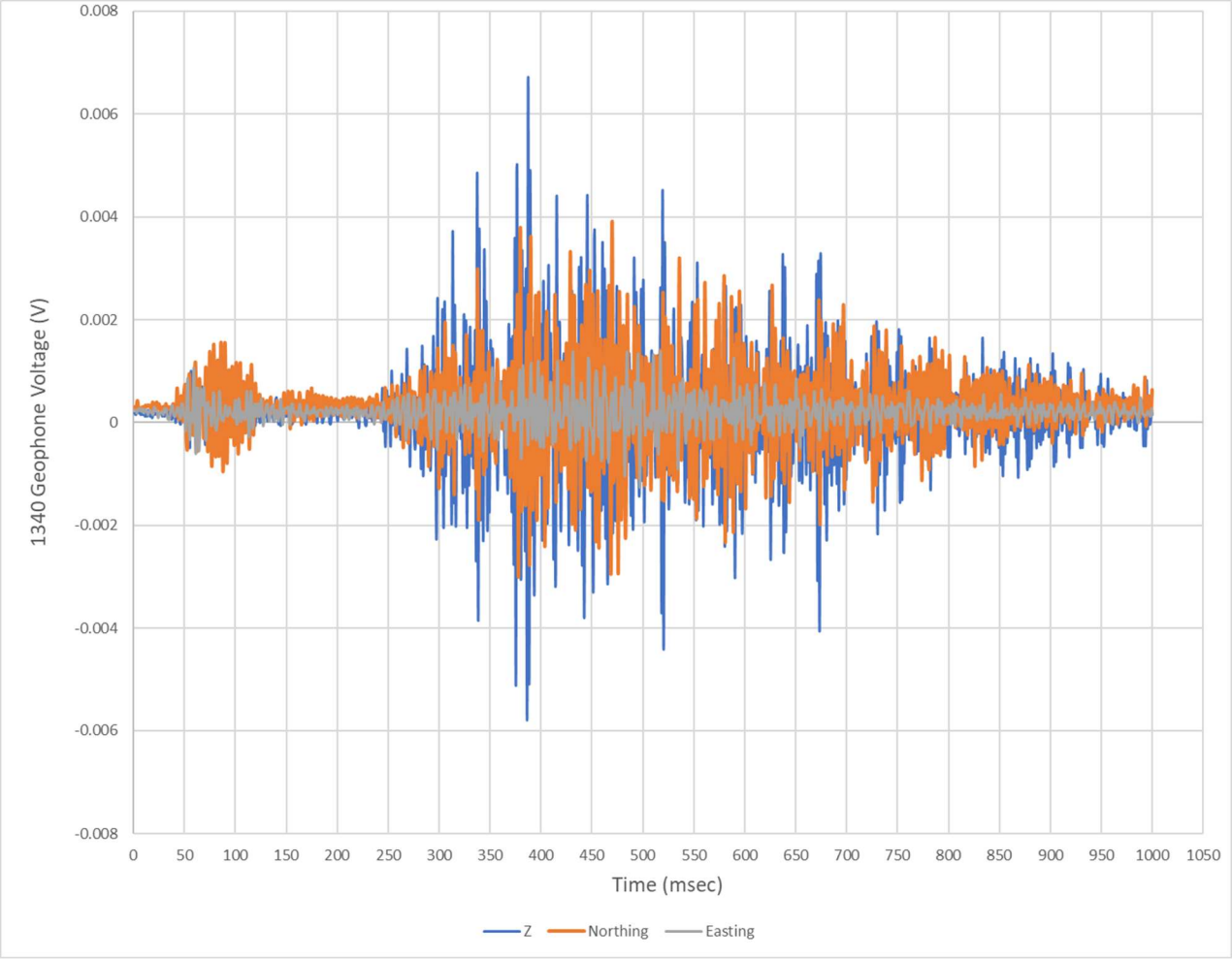

Figure 28 IDAQ geophone recording of a detonator check test. The elastic and air wave phases are apparent

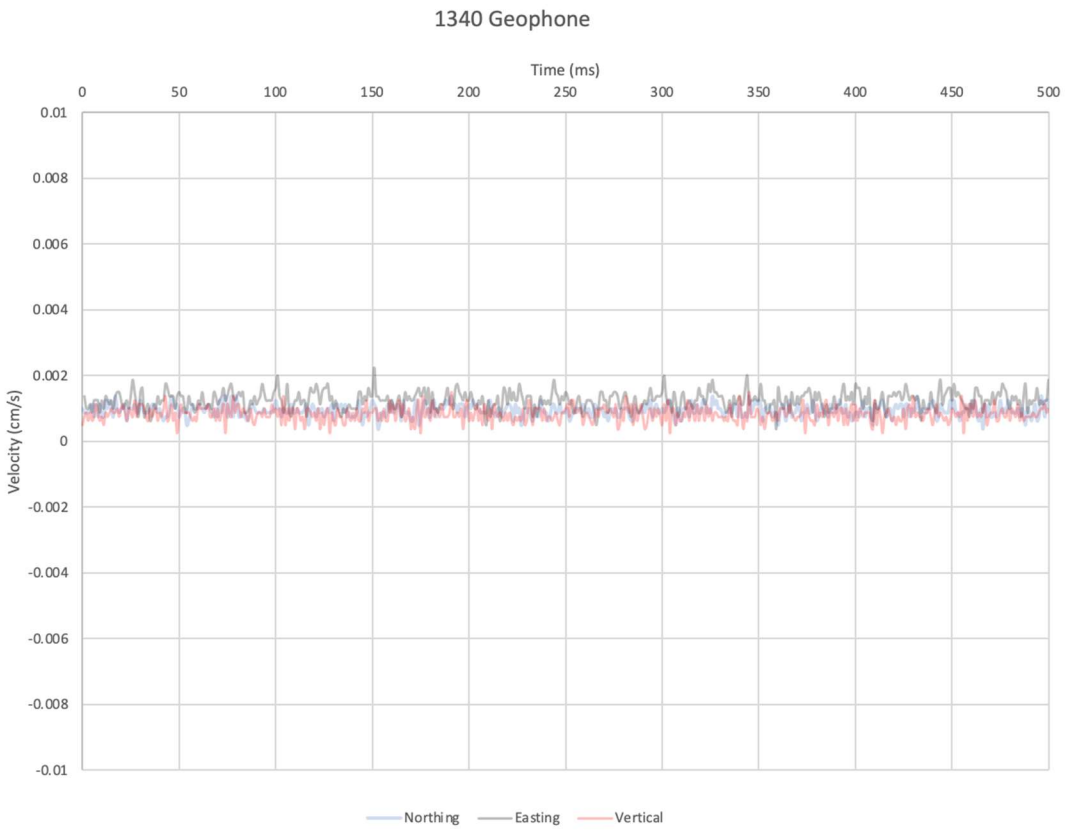

Figure 29 IDAQ geophone noise recording at 1340 location

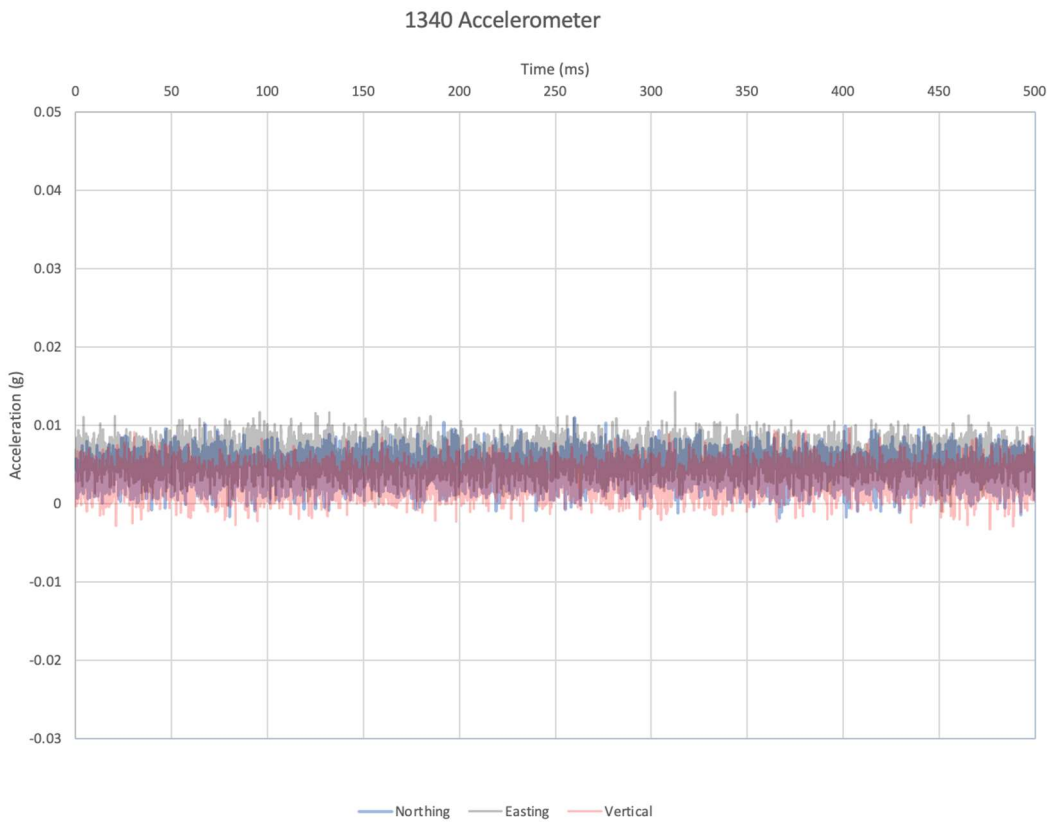

Figure 30 IDAQ accelerometer noise recording at 1340 location

Figure 31 IDAQ geophone noise recording at Walker location

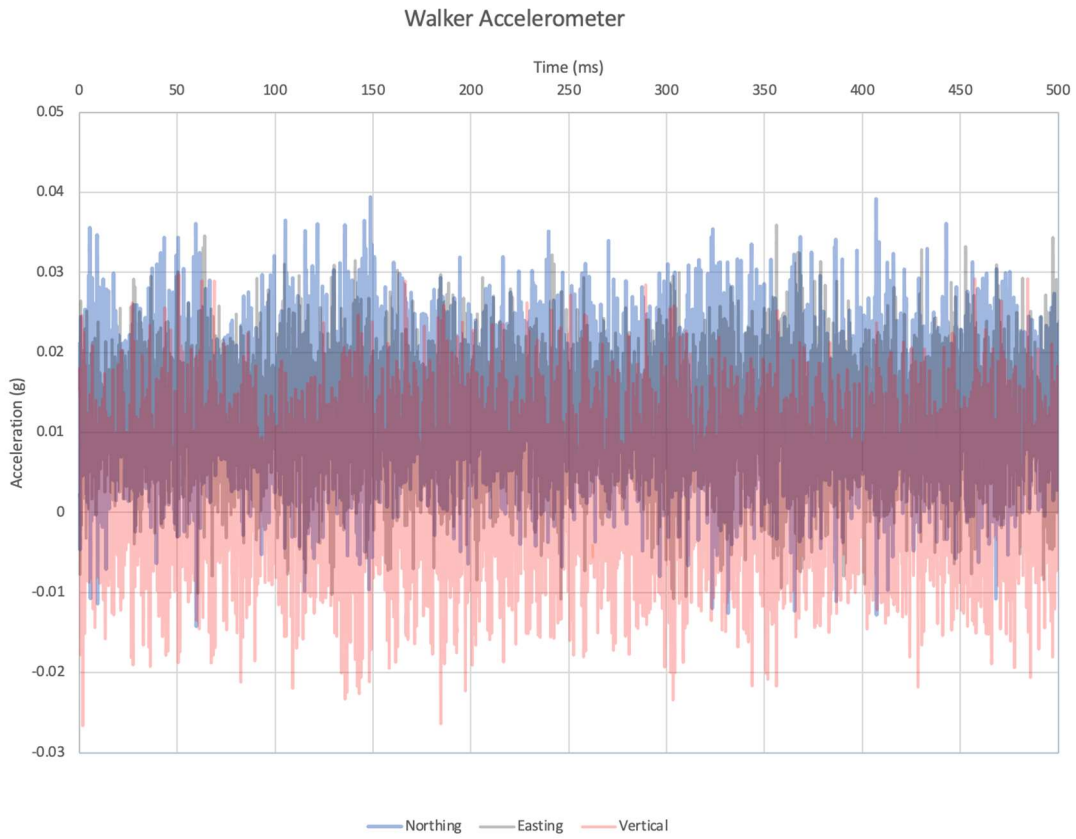

Figure 32 IDAQ accelerometer noise recording at Walker location

3.2.6 Drift Environmental Conditions

In addition to shock induced damage, high humidity or temperature conditions can lead to failure of sensitive IDAQ electronic equipment. The IDAQ enclosures were not designed to be water or gas tight, but sufficiently resistant to ingress, so that desiccant packs would be able to maintain acceptably low humidity levels (<75% RH) and were replaced approximately every three months. The IDAQ thermal managed system was also appropriately sized to remove the heat load generated by the enclosed equipment. Humidity and temperature were continuously monitored and recorded and never exceeded the alarm thresholds at any time during the experiment.

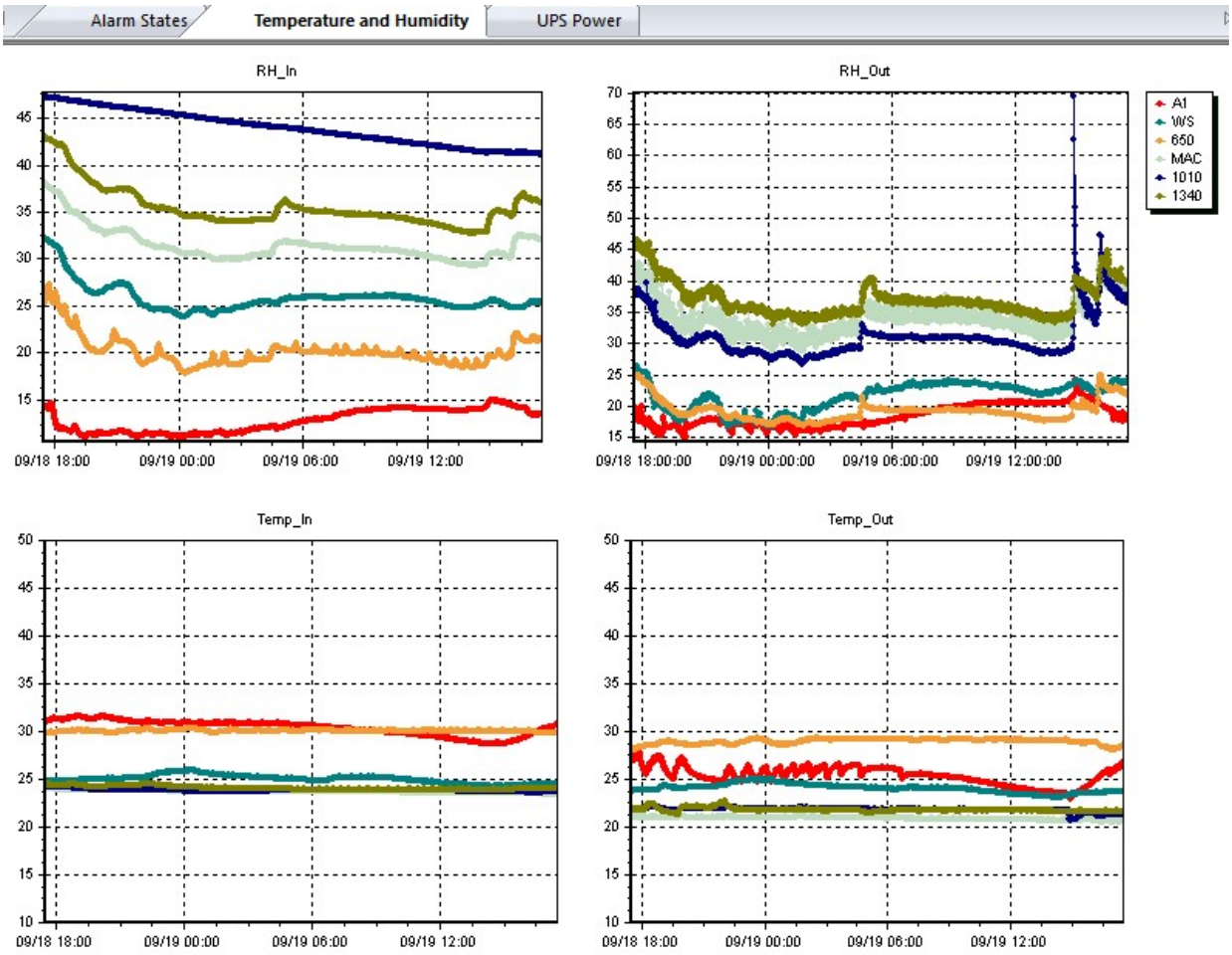

Figure 33 IDAQ environmental conditions monitoring GUI

3.2.7 Electromagnetics

Electromagnetic interference (EMI) can be expected in an industrial underground environment and vary both temporally and spatially within the facility. Investigations were performed on several occasions to quantify and document the EM noise conditions in P.06 bypass drift. Recordings of the EM sensors at both the 1010 and 650 locations were collected at various times (Figure 34). In addition, a campaign was undertaken to identify EMI sources throughout the P.06 bypass using a portable sensor and oscilloscope to determine if specific issues could be identified and mitigated. Elevated EM noise conditions were found in several locations relative to less noisy locations (Figure 35), particularly where additional instrumentation (Figure 36) or power systems (Figure 37) were located. The noise contained 60Hz and higher harmonics as well as other signatures likely due to switch mode power supplies and UPS charging systems.

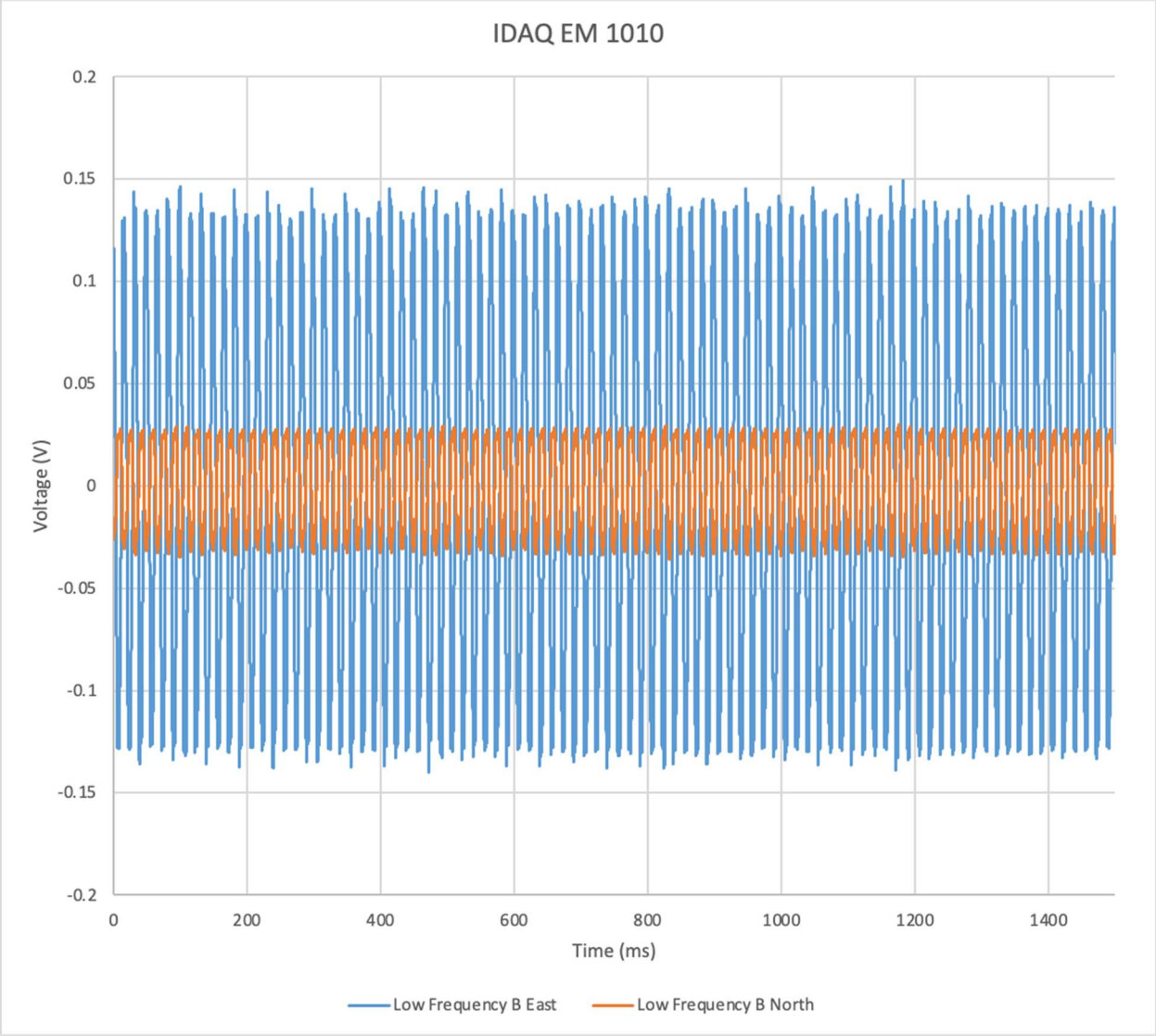

Figure 34 EM noise recording by 1010 IDAQ prior to the explosive experiment

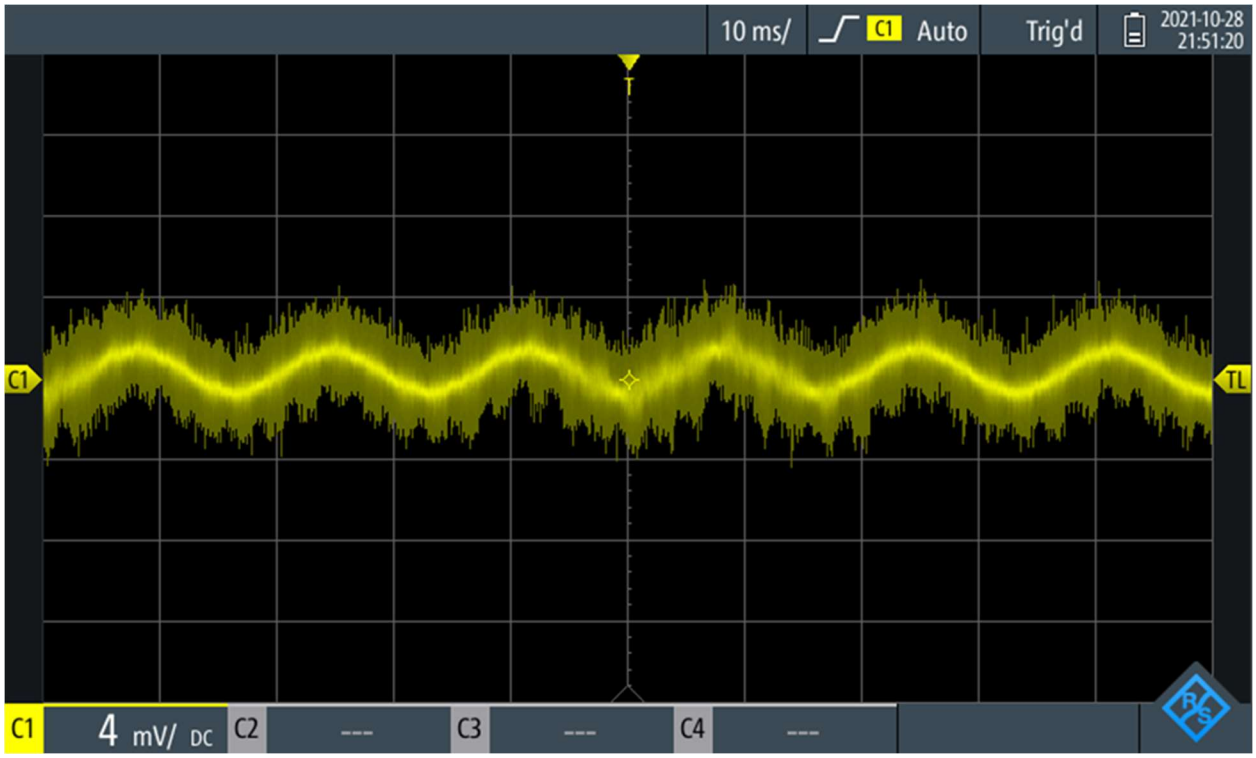

Figure 35 Time domain recording of noise in the 1010 facility

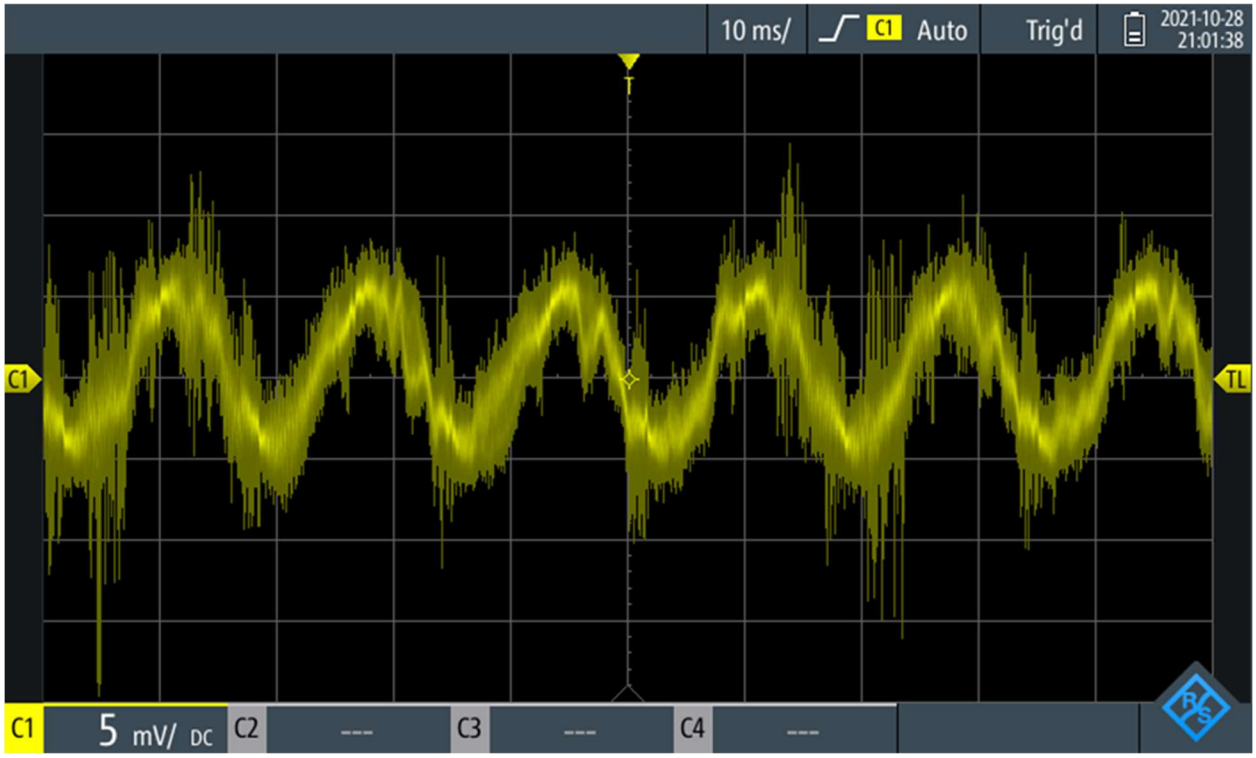

Figure 36 Time domain recording of noise in the 650 facility

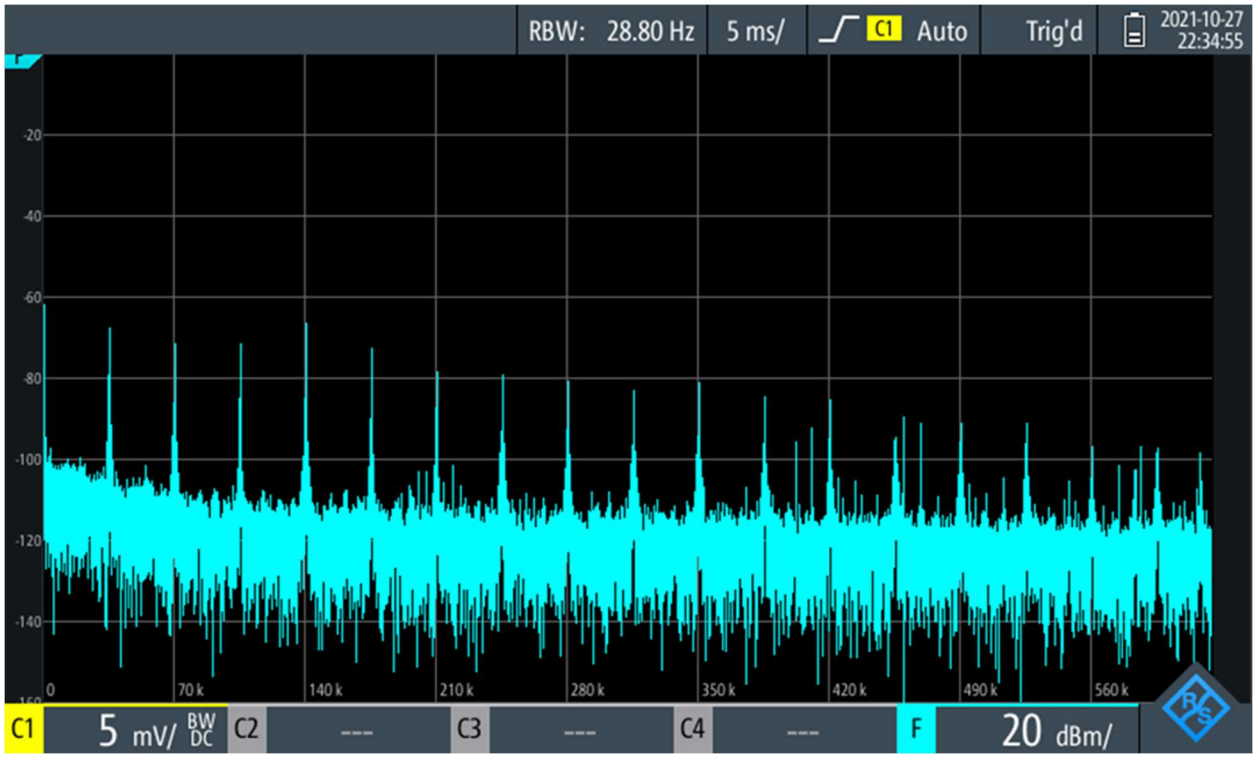

Figure 37 Frequency domain noise spectrum on instrumentation cables located on the left rib of the P.06 bypass drift near 1100 power center

4.0 Experiment A - IDAQ Observations

4.1 General Performance Observations

The first in the series of PE1 explosive experiments was conducted at 15:15:00 UTC on October 18th, 2023. All prompt sensors (cavity pressure and temperature, accelerometers, geophones, electromagnetic, and distributed acoustic) recorded data during and immediately after the explosion. Explosive by-product gases and those introduced to the stack as tracers were transported into the P.06 bypass drift within minutes and were monitored by the various gas analysis instrumentation systems for several weeks.

Throughout the entire experiment the IDAQ system performed well and recorded all data as expected. No upset or unusual conditions relating to data exfiltration, remote instrument control, or data backup occurred.

4.2 Ground Motion

Initial ground motion from the explosion was observed by both geophones and accelerometers at all IDAQ locations. Geophone data (after time differencing the measured velocities) were consistent with accelerometer data recorded at each location (Figure 38).

The time observed for energy to first arrive were handpicked from both geophone and accelerometer data at each IDAQ location. A plot of the move out indicates that the average P-wave velocity was approximately 2.5km/s in the media surrounding the experiment (Figure 39). Similar data recorded during the detonator checks prior to the experiment suggested the P-wave velocity was lower, approximately 2.0 km/s, but this dataset was limited by much weaker ground motion signals and was observed only on the 1340 and 1010 geophones.

Peak velocities and accelerations observed during the explosion were also determined from data collected by the respective IDAQ geophone and accelerometer arrays (Figure 40). All sensors recorded the event well with one possible exception being that the closest geophone at 1340 may have clipped. Peak ground motions were observed to fall off with distance following empirical relationships established for historical tests on the NNSS [Murphy and Lahoud 1969; Perret and Bass 1975].

Hundreds of aftershocks were recorded by both the IDAQ geophones (Figure 41 and Figure 42) and DAS within the first day following the explosion. Most of the events occurred in the first 24 hours after the explosions; the number of events observed after that time was small. Initial analysis of aftershock event decay rates for experiment A may suggest differences between PE1-A observations and historical data [Ford and Walter 2010] but additional work is needed to verify.

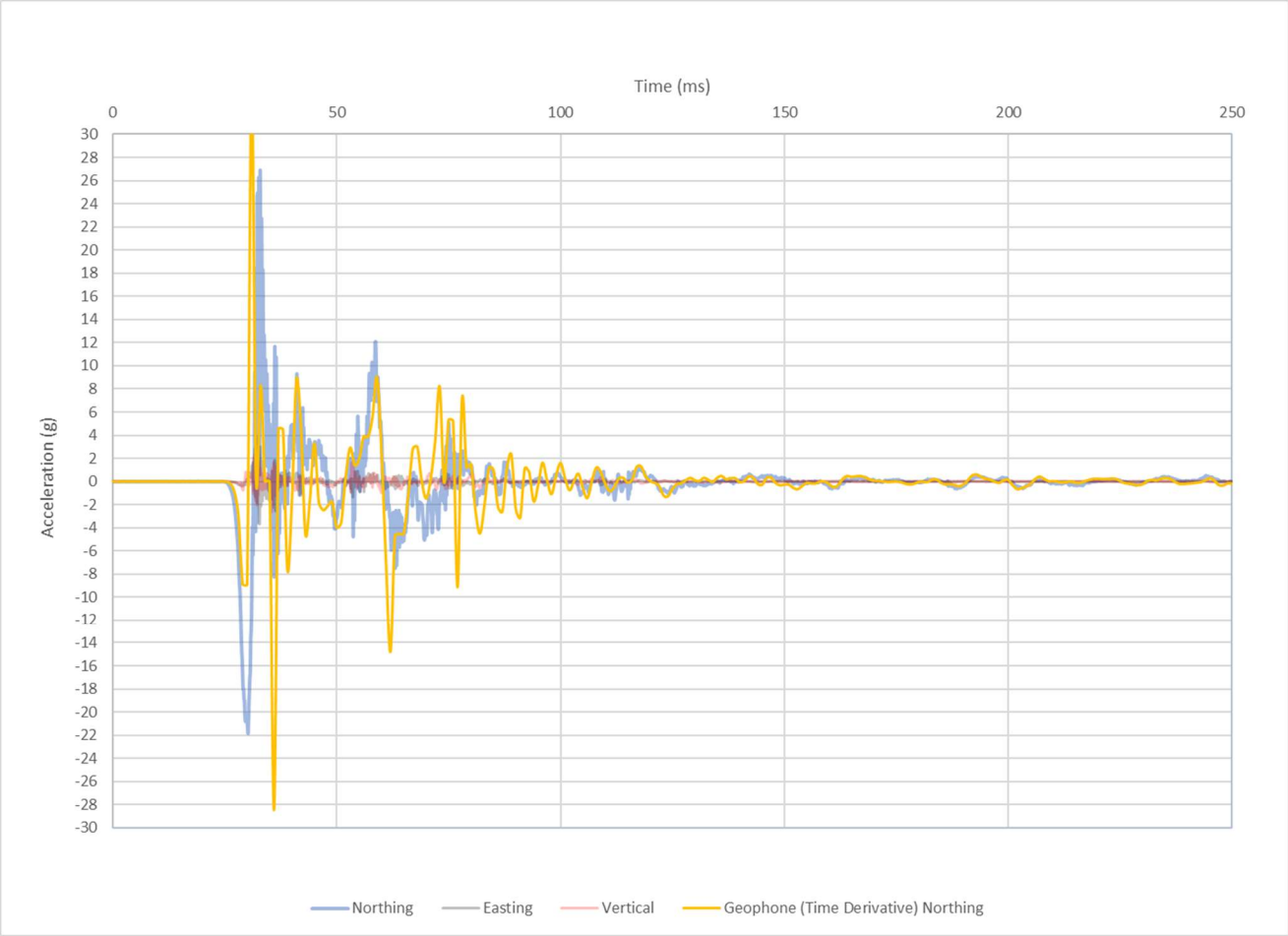

Figure 38 IDAQ accelerometer and time differenced geophone data recorded during the explosion

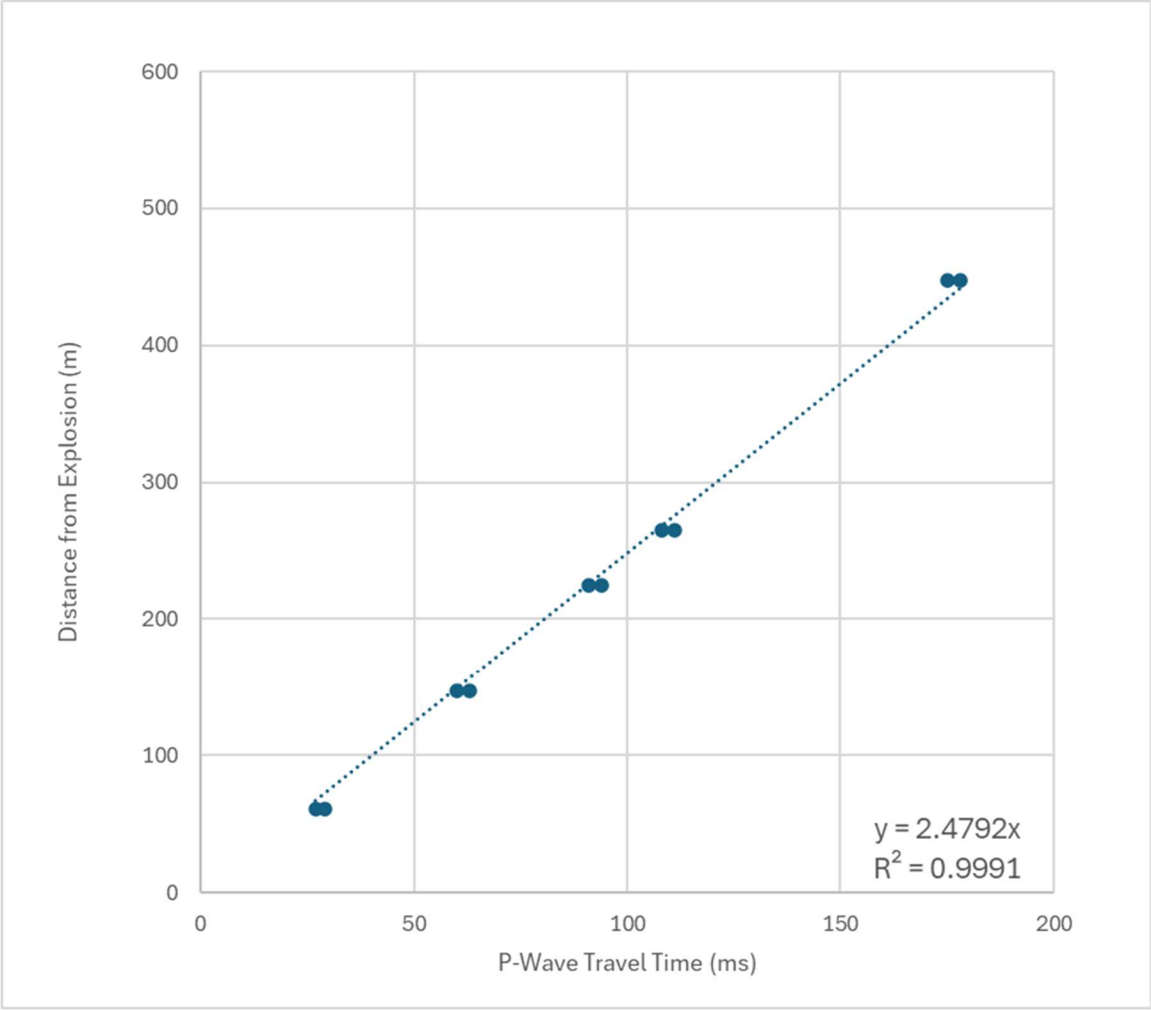

Figure 39 Plot of first arriving energy times recorded at all IDAQ geophones and accelerometers. Linear fit of move out indicates a P-wave velocity of approximately 2.5 km/s

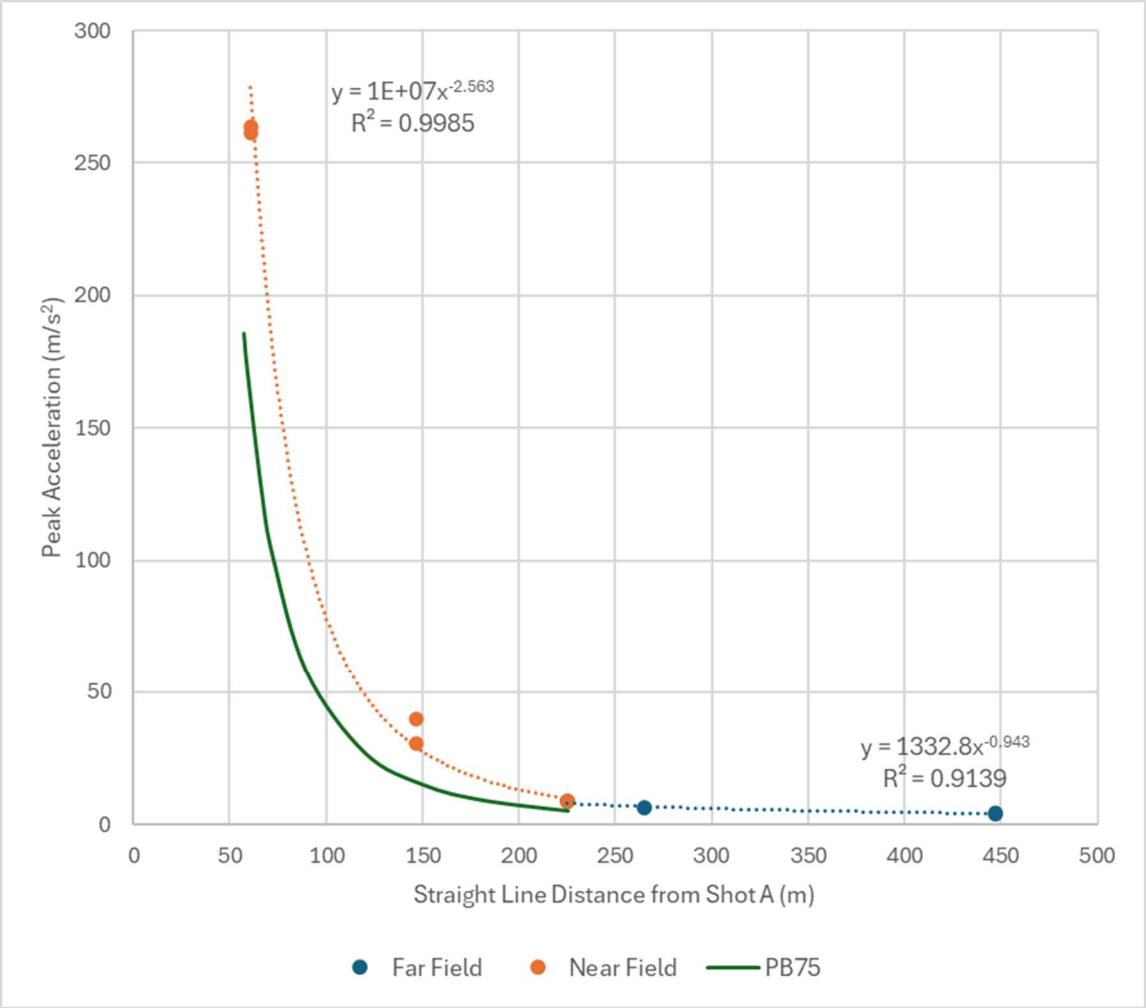

Figure 40 Plot of peak accelerations recorded on all IDAQ ground motion sensors

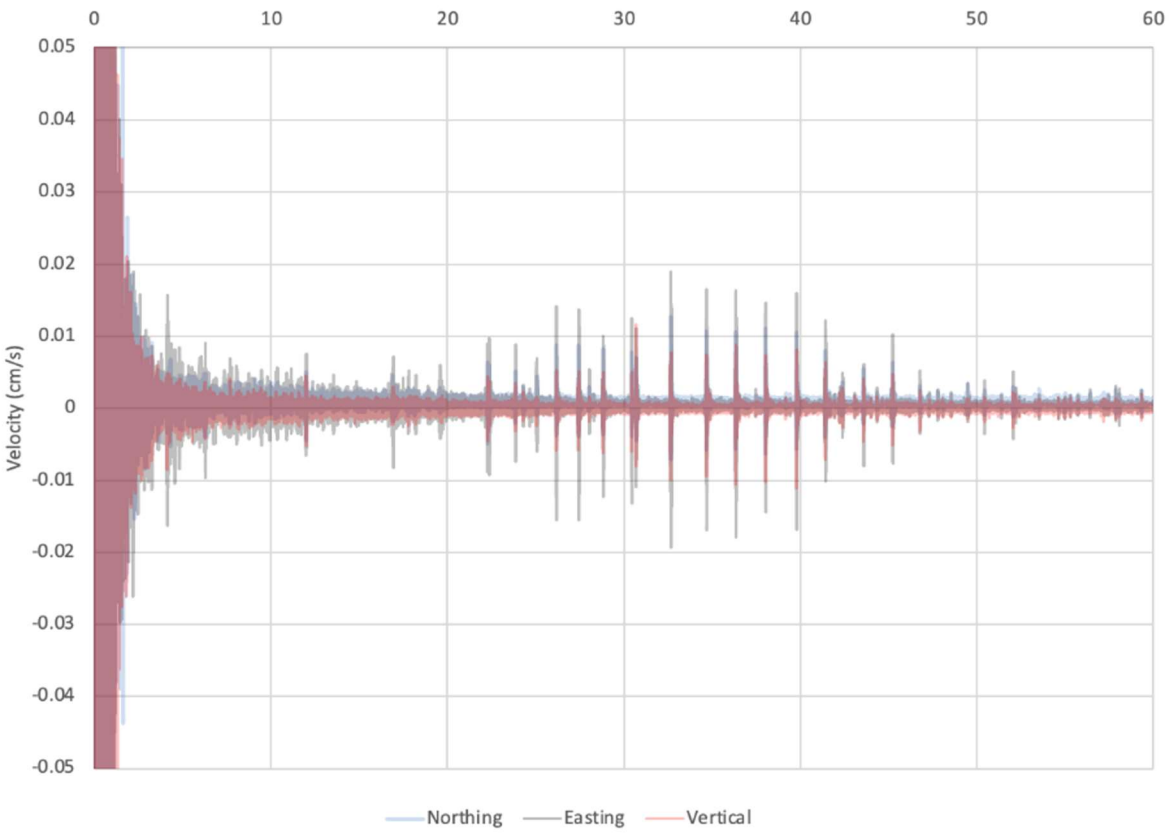

Figure 41 Aftershocks recorded on the IDAQ geophone at 1340 in the first 60 seconds

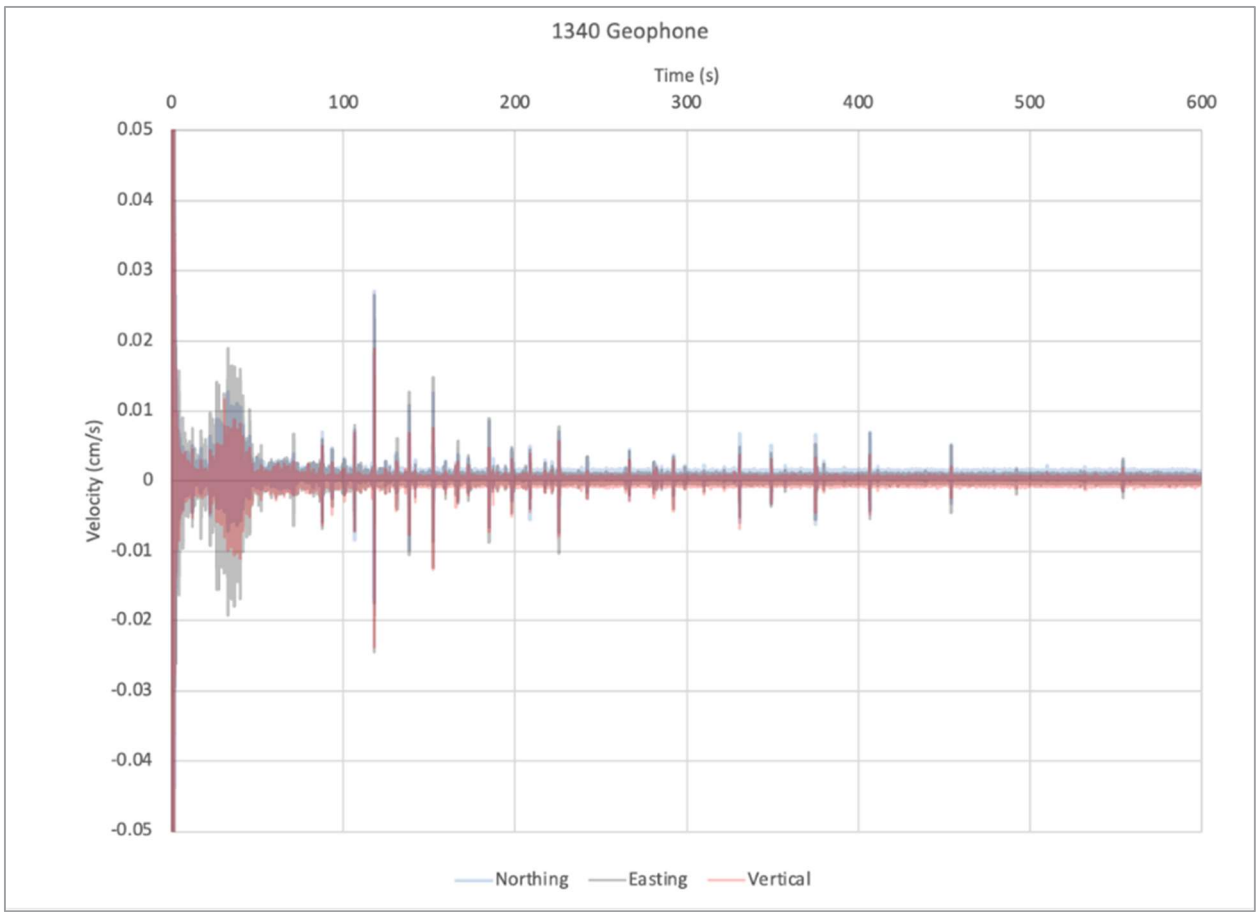

Figure 42 Aftershocks recorded on the IDAQ geophone at 1340 in the first 10 minutes after the explosion

4.3 Drift Environmental Conditions

High gas concentrations were expected and observed but no detrimental effects to the IDAQ occurred. The network of IDAQ cameras successfully captured motion of the grout plug that contained the explosion. A set of lights were attached to the face of the grout plug to aid in camera monitoring (Figure 43). Both images (automatically captured and recorded approximately every minute) and movies were collected by all the cameras prior to the experiment. During the experiment a movie clip using the camera facing the experimental drift plug at 1490 was recorded at the maximum rate (60 frames per second) and captured several interesting features such motion of the grout plug and several minor structural elements that moved. Following the experiment, images recorded changes that indicated only minor damage to the surrounding area.

Figure 43 Camera image of the experiment grout plug and surrounding area prior to the experiment

Figure 44 Camera image of the experimental grout plug and surrounding area during the explosion

Figure 45 Camera image of the experimental grout plug and surrounding area following the explosion

4.4 Electromagnetics

The PE1 electromagnetics instrumentation team installed an array of E-field and B-field sensors both in the P.06 bypass drift and on the mesa above the U12 P-tunnel facility. All the sensors successfully recorded EM signals from the explosion. As mentioned previously, the week prior to the experiment the DAQ at the 1010 facility failed and the IDAQ node there was modified to acquire the low frequency E-field and B-field sensor data.

The working hypothesis for this experiment was that the EM signals would be the result of a magnetic bubble effect [Malik et al 1985]. Initial analysis of observations from all PE1 EM sensors (Figure 46) suggest that another source mechanism may be at work. Additional analysis and future experiments may shed more light on this finding.

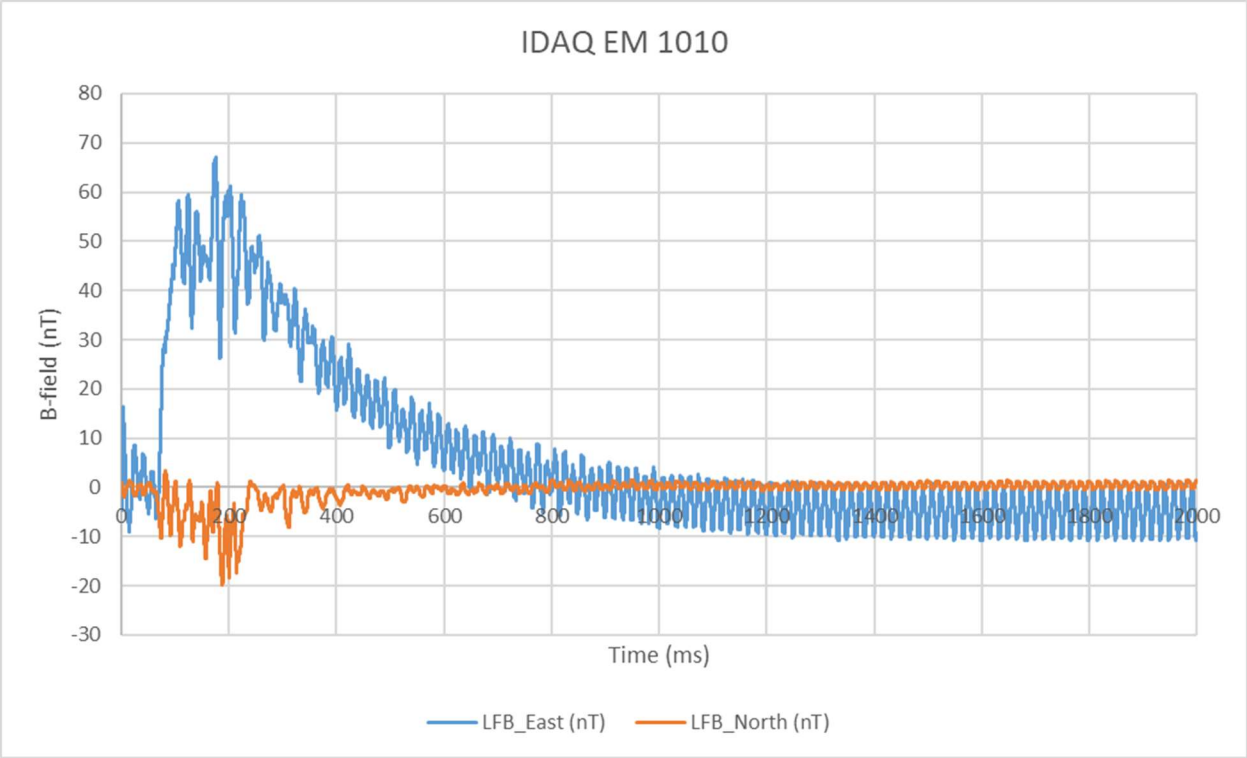

Figure 46 B-field recorded during the explosion by the IDAQ at 1010

5.0 Lessons Learned and Modifications for Future Experiments

In all, the PE1-A experiment yielded a rich dataset that can be used by researchers now and in the future. While nearly all instrumentation systems performed quite well, a few modifications intended to improve the overall design are recommended:

- The trigger fiber optic link between 1340 and the apron is very long and near the limits of the optical-electrical system. Adding a new node in P-main will make the connection more robust
- Higher speed camera pointing at the experimental drift bulkhead could provide improved data on drift plug motion
- Humidity and temperature were located too close to IDAQ node enclosures and partially sensed the interior conditions. Sensor should be moved further outside the enclosure and placed in a protective housing mounted to the rib.
- Monitoring of additional explosive gas byproducts will help to better understand gas migration in the drift and assist with operational decisions
- Additional subsurface ground motion and EM sensing to improve spatial coverage (azimuthal and distance) that could lead to better aftershock locations, relationships between yield-distance-ground motion, co-located DAS interpretation, and EM source mechanisms validation

6.0 References

Myers S.C. et al. 2024. A Multi-Physics Experiment for Low-Yield Nuclear Explosion Monitoring. Lawrence Livermore National Laboratory Report. LLNL-TR-864107

Murphy, J.R. & Lahoud, J.A., 1969. Analysis of seismic peak amplitudes from underground nuclear explosions, Bull. seism. Soc. Am., 59(6), 2325–2341

Perret, W.R. & Bass, R.C., 1975. Free-field ground motion induced by underground explosions, No. SAND-74-0252, Sandia Labs., Albuquerque, NM, USA

Ford, S.R., and W.R. Walter. 2010. Aftershock Characteristics as a Means of Discriminating Explosions from Earthquakes, Bull. Seis. Soc. Amer., 100, 364–376, doi:10.1785/0120080349

Malik, J, Fitzhugh, R, and Homuth, F. 1985. Electromagnetic signals from underground nuclear explosions. Los Alamos National Laboratory Report. LA-10545 MS

Appendix A – IDAQ Components

Table 2 IDAQ node components

Component description	Manufacturer	Model
RAID drive	Synology	SAMZ76P4T0BW
Ethernet Switch	Cisco	IE-4000-16GT4G-E/ IE-4000-8GT4G-E
AC/DC Power Converter	Cisco	PWR-IE50W-AC-IEC
ROTOMold Enclosure	SKB	3SKB-R06U20W
Fiber Ports	Siemon	XG2-XLC-LC-SM
Ethernet Ports	Amphenol	523-RJF6A2A1RAB
PTP clock	Masterclock	GMR5000
UPS	Tripplite	SU2200RTXL2U
UPS Power Relay	Tripplite	SU3000RTXL2U
Enclosure A/C	Rittal	3201200
Optical to Electrical Converters	Highland Technologies	J730
Electrical to Optical Converters	Highland Technologies	J720
SRS Trigger Distribution Amplifier	Stanford Research Systems	FS735
High Frequency DAQ	National Instruments	cRIO-9045
Geophone/Accelerometer cRIO modules	National Instruments	NI-9234
Trigger cRIO module	National Instruments	NI-9402
Campbell data logger	Campbell Scientific	CR310
DC Power Supply	Eaton	PSG960R24RM
Accelerometer	PCB Piezotronics	356A25
Geophone	OYO Geospace	GS-20DM
Temperature/Relative Humidity Sensor	Campbell Scientific	HMP60

Table 3 IDAQ sensors

Channel Description	Orientation	Manufacturer	Sensor Type	Model	Sensor Range	Sensitivity
State-of-Health ground motion monitoring	Easting	PCB Piezotronics	Accelerometer	356A series	0-400g	10 - 100 mV/g
State-of-Health ground motion monitoring	Northing	PCB Piezotronics	Accelerometer	356A series	0-400g	10 - 100 mV/g
State-of-Health ground motion monitoring	Vertical	PCB Piezotronics	Accelerometer	356A series	0-400g	10 - 100 mV/g
State-of-Health ground motion monitoring	Easting	OYO Geospace	Geophone	GS-20DM	0.203cm max displacement	24.4 V/m/s (60% damping)
State-of-Health ground motion monitoring	Northing	OYO Geospace	Geophone	GS-20DM	0.203cm max displacement	24.4 V/m/s (60% damping)
State-of-Health ground motion monitoring	Vertical	OYO Geospace	Geophone	GS-20DM	0.203cm max displacement	24.4 V/m/s (60% damping)
State-of-Health internal temperature monitoring	N/A	Vaisala	Thermistor	HMP60	-40 - 60C	0.6C
State-of-Health external temperature monitoring	N/A	Vaisala	Thermistor	HMP60	-40 - 60C	0.6C
State-of-Health internal relative humidity monitoring	N/A	Vaisala	Thermistor	HMP60	0-100% RH	5% RH
State-of-Health external relative humidity monitoring	N/A	Vaisala	Thermistor	HMP60	0-100% RH	5% RH
State-of-Health UPS-power monitoring	N/A	Tripplite	UPS Power Relay	SU3000RTXL2U	Switch closure	N/A

PNNL-37567

Pacific Northwest National Laboratory

902 Battelle Boulevard
P.O. Box 999
Richland, WA 99354
1-888-375-PNNL (7665)

www.pnnl.gov